

# The EWMA Sign Chart Revisited: Performance and Alternatives without and with Ties

Theodoros Perdikis <sup>a</sup>, Stelios Psarakis <sup>a</sup>, Philippe Castagliola <sup>b</sup>, Athanasios C. Rakitzis <sup>c</sup>, Petros E. Maravelakis <sup>d</sup>

<sup>a</sup>Department of Statistics & Laboratory of Statistical Methodology, Athens University of Economics and Business Athens, Greece; <sup>b</sup>Université de Nantes & LS2N UMR CNRS 6004, Nantes, France; <sup>c</sup>Department of Statistics & Actuarial-Financial Mathematics, University of the Aegean, Karlovasi, Greece; <sup>d</sup>Department of Business Administration, University of Piraeus, Piraeus, Greece

## ARTICLE HISTORY

Compiled December 14, 2022

## ABSTRACT

The EWMA Sign control chart is an efficient tool for monitoring shifts in a process regardless the observations' underlying distribution. Recent studies have shown that, for nonparametric control charts, due to the discrete nature of the statistics being used (such as the Sign statistic), it is impossible to accurately compute their Run Length properties using Markov chain or integral equation methods. In this work, a modified nonparametric Phase II EWMA chart based on the Sign statistic is proposed and its *exact* Run Length properties are discussed. A continuous transformation of the Sign statistic, combined with the classical Markov Chain method, is used for the determination of the chart's in- and out-of-control Run Length properties. Additionally, we show that when ties occur due to measurement rounding-off errors, the EWMA Sign control chart is no longer distribution-free and a Bernoulli trial approach is discussed to handle the occurrence of ties and makes the proposed chart almost distribution-free. Finally, an illustrative example is provided to show the practical implementation of our proposed chart.

**Keywords:** Nonparametric control chart, Sign statistic, Markov chain, EWMA control chart, Rounding-off errors.

## 1. Introduction

Control charts are one of the major tools of Statistical Process Monitoring (SPM), a technique which plays a vital role in manufacturing industries. They can be used for the monitoring of a process in real-time, aiming to identify possible assignable causes in it quickly and accurately. The most well-known control charts are the Shewhart-type control charts introduced by Shewhart in [27]. Shewhart charts are suitable for detecting sudden, and of large magnitude, shifts in process parameters. However, when the changes in process parameters are of small to moderate magnitude, Cumulative Sum (CUSUM, see [22]) and Exponentially Weighted Moving Average (EWMA, see [26]) charts are preferable than Shewhart charts. Because of their

memory-type property, CUSUM and EWMA charts are known to react more quickly than Shewhart charts. It is worth stretching that for the design of CUSUM and EWMA charts, we assume that the distribution of the observations collected at each sampling point, is known. However, practitioners usually do not have an a priori information about the distribution of the monitored characteristic. As a consequence, a new class of control charts has been proposed, known as nonparametric (or distribution-free) control charts, capable of monitoring shifts in process parameters without any knowledge of the observations' underlying distribution. A detailed review of existing univariate and multivariate distribution-free control charts can be found in [7]. Over the past two decades, the design of nonparametric EWMA-type schemes has drawn the researchers' attention introducing EWMA charts based on popular nonparametric statistics, like the Sign statistic (see, [2, 13, 15, 25, 29]) or the Wilcoxon Signed Rank or Rank-Sum statistic (see [1, 8, 14]).

In general, for EWMA and CUSUM-type schemes, in the case of monitoring observations from a continuous distribution, a reliable approximation of their RL (Run Length) properties such as the ARL (Average Run Length), and the SDRL (Standard Deviation Run Length) can be obtained by using the Markov chain method of Brook and Evans presented in [3]. Recently, Wu et al. (see, [28]) noticed that the method of Brook and Evans [3] is not always an efficient technique for computing the RL properties of a distribution-free EWMA control chart. In particular, since the distribution of the statistics that are being used (for example the sign statistic) is a discrete one, it is not always possible to compute *exactly* the in-control and the out-of-control ARL (to be denoted as  $ARL_0$ ,  $ARL_1$ , respectively) by using this approach. In order to tackle this problem, Wu et al. in [28], proposed a new method, known as the "continuousify" method, for calculating the RL properties of an EWMA chart for count data. According to this method, the initial discrete random variables (count data) are transformed into continuous ones, which are a mixture of normally distributed random variables. Similarly, Perdakis et al. in [23], using the "continuousify" method presented in [28], proposed a modified one-sided distribution-free EWMA chart based on Signed Ranks and derived its exact in- and out-of-control RL properties.

It should be noted that besides the use of reliable metrics regarding the efficient evaluation of the chart's performance, the accuracy of the measurement system also plays a vital role in its design phase. Over the past decades, the investigation of conventional control charts (i.e charts assuming normality) under measurement errors has drawn the researchers' interest in particular with reference to the bias and precision errors which introduce a rounding-off error resulting in a discretization of the observed measures. For a detailed literature review of control charts under measurement errors the reader is referred to Maleki et al. in [18]. It is worth stretching that, rounding-off errors often result in "ties", even if their true distribution is continuous. Generally, in nonparametric statistical inference the treatment of ties is of high importance due to the fact that the distribution of the nonparametric statistics such as the Sign or the Wilcoxon signed rank statistics is seriously affected by the presence of ties([11, 12, 24]). As far as we know there are few publications related with the effect of the measurement error in nonparametric control charts. Castagliola et al. in [4] investigated the performance of the Shewhart Sign control chart under measurement error scenarios. Recently, Nojavan et al. in [21] examined the effect of the measurement error on the performance of Shewhart control charts, based on the

Mann-Whitney and Signed-Rank statistics.

In this work, using the methodology of Wu et al. presented in [28], a new EWMA control chart based on the Sign statistic chart is proposed and its *exact* RL properties are computed. Additionally, its distribution-free property under measurement errors is investigated and procedures to handle the occurrence of ties are discussed. The paper is structured as follows: In Section 2, an extended version of the distribution-free EWMA Sign chart originally introduced by Graham et al. in [13] is proposed (to be denoted as the C-SN EWMA chart) and its exact RL properties are evaluated via the “continuousify” method. In addition, the efficiency of the “continuousify” method is investigated and the chart’s optimal parameters ( $\lambda^*$ ,  $K^*$ ) are presented under several scenarios. In Section 3, the distribution of the Sign statistic is defined when ties exist. In Section 4, our proposed C-SN EWMA chart “with ties” is defined and the effect of the measurement system resolution is examined. Additionally, we discuss procedures to tackle the occurrence of rounding-off errors. In Section 5 an illustrative example is discussed to show the practical implementation of the operation of our proposed chart when ties are present. Finally, some concluding remarks and suggestions for future work are presented in Section 6.

## 2. The EWMA Sign chart without ties

Graham et al. in [13] introduced a new nonparametric two-sided EWMA chart based on the Sign statistic and, using the Markov-Chain approach of Brook and Evans presented in [3], obtained its optimal design parameters and investigated its out-of-control performance under several distributions.

Suppose that, at each sampling point  $t = 1, 2, \dots$ , a subgroup  $\{X_{t,1}, X_{t,2}, \dots, X_{t,n}\}$  of size  $n$  following an unknown continuous distribution with c.d.f. (cumulative distribution function)  $F_X(x|\theta)$  is collected where  $\theta$  is the location parameter to be monitored. If  $\theta = \theta_0$  the process is declared as in-control and, if  $\theta = \theta_1$ , the process is declared as out-of-control. In this work, we consider  $\theta$  as being the median of the distribution. The two-sided EWMA chart based on the Sign statistic is defined by the following formulas:

$$SN_t = \sum_{j=1}^n S_{t,j},$$

$$Z_t = \lambda SN_t + (1 - \lambda)Z_{t-1}, Z_0 = E_0(SN_t), \quad (1)$$

where  $E_0(SN_t)$  is the in-control expectance of  $SN_t$  and  $S_{t,j} = \text{sign}(X_{t,j} - \theta_0)$  with  $\text{sign}(x) = -1, 0$  or  $+1$  if  $x < 0, x = 0$  or  $x > 0$ , respectively. Moreover, let  $\mathbf{p} = (p_{-1}, p_0, p_{+1})$  be the vector of probabilities:

$$\begin{aligned}
p_{-1} &= P(S_{t,j} = -1) = P(X_{t,j} < \theta_0) = F_X(\theta_0|\theta), \\
p_0 &= P(S_{t,j} = 0) = P(X_{t,j} = \theta_0), \\
p_{+1} &= P(S_{t,j} = +1) = P(X_{t,j} > \theta_0) = 1 - F_X(\theta_0|\theta).
\end{aligned}$$

It should be noted that, the assumption of having samples from a *continuous* distribution, prevents to have tied pairs for  $X_{t,j}$  and  $\theta_0$  and so, the event  $S_{t,j} = 0$  is not possible to occur. As a consequence,  $S_{t,j}$  can be either  $+1$  or  $-1$  and we have  $p_0 = 0$  and  $p_{-1} = 1 - p_{+1}$ . The theoretical properties of  $SN_t$  can be derived by taking into account that  $SN_t$  is defined on  $\{-n, -n+2, \dots, n-2, n\}$  and its distribution can be derived from the relationship  $SN_t = 2D_t - n$ , where  $D_t$  is the number of observations  $\{X_{t,1}, X_{t,2}, \dots, X_{t,n}\}$  larger than  $\theta_0$ . Therefore, since  $p_{+1} = P(X_{t,j} > \theta_0)$ ,  $D_t$  is a binomial random variable with parameters  $n$  and success probability  $p_{+1}$ . As a consequence, the c.d.f.  $F_{SN_t}(s|n, p_{+1})$  of  $SN_t$  is equal to

$$F_{SN_t}(s|n, p_{+1}) = F_{\text{Bin}}\left(\frac{n+s}{2} | n, p_{+1}\right), \quad (2)$$

where  $s \in \{-n, -n+2, \dots, n-2, n\}$  and  $F_{\text{Bin}}(\dots | n, p_{+1})$  is the c.d.f. of the binomial distribution which depends on the sample size  $n$  and  $p_{+1}$ . Additionally, when the process is in-control  $p_{-1} = p_{+1} = 0.5$ , and so the c.d.f. of  $SN_t$  reduces to:

$$F_{SN_t}(s|n, 0.5) = F_{\text{Bin}}\left(\frac{n+s}{2} | n, 0.5\right).$$

Using the relationship between  $SN_t$  and  $D_t$ , the expectance and variance of  $SN_t$  are equal to

$$\begin{aligned}
E(SN_t) &= 2E(D_t) - n = 2np_{+1} - n, \\
V(SN_t) &= 4V(D_t) = 4np_{+1}(1 - p_{+1}).
\end{aligned}$$

For the in-control case, since  $p_{-1} = p_{+1} = 0.5$ , the in-control expectance  $E_0(SN_t)$  and variance  $V_0(SN_t)$  of  $SN_t$  are simply defined as:

$$\begin{aligned}
E_0(SN_t) &= 0, \\
V_0(SN_t) &= n.
\end{aligned}$$

Therefore, the asymptotic upper and lower control limits of the two-sided SN EWMA chart are obtained by using the following classical formulas (see,[7])

$$\begin{aligned}
\text{LCL} &= E_0(SN_t) - K \sqrt{V_0(SN_t)} \times \sqrt{\frac{\lambda}{2-\lambda}}, \\
\text{UCL} &= E_0(SN_t) + K \sqrt{V_0(SN_t)} \times \sqrt{\frac{\lambda}{2-\lambda}}.
\end{aligned}$$

If we consider the in-control values  $E_0(\text{SN}_t)$  and  $V_0(\text{SN}_t)$ , the asymptotic upper and lower control limits simply reduce to

$$\begin{aligned} \text{LCL} &= -K\sqrt{\frac{n\lambda}{2-\lambda}}, \\ \text{UCL} &= K\sqrt{\frac{n\lambda}{2-\lambda}}. \end{aligned}$$

### 2.1. Performance

For EWMA-type schemes, the techniques that are commonly used for the computation of their ARL and SDR are the Markov chain method of Brook and Evans ([3]) and the method of integral equations (Crowder [10]). Champ and Rigdon [9] compared and showed that these two methods are actually equivalent when used with the EWMA chart. Here, we proceed with the Markov chain method because it has been widely used for the computation of the RL properties of nonparametric EWMA-type charts. The method of Brook and Evans in [3], assumes that the operation of the EWMA control chart can be well represented by a discrete-time Markov chain where the control limit interval  $[\text{LCL}, \text{UCL}]$  is divided into  $2m + 1$  subintervals of width  $2\Delta$  where  $\Delta = \frac{\text{UCL}-\text{LCL}}{4m+2}$ . Moreover, let  $H_j = \frac{\text{LCL}+\text{UCL}}{2} + 2j\Delta$  be the  $j$ -th midpoint of state  $j = \{-m, \dots, 0, \dots, m\}$ . The transition probability matrix  $\mathbf{P}$  for the two-sided SN EWMA chart is defined as:

$$\mathbf{P} = \begin{pmatrix} \mathbf{Q} & \mathbf{r} \\ \mathbf{0}^\top & 1 \end{pmatrix} = \begin{pmatrix} Q_{-m,-m} & \cdots & Q_{-m,-1} & Q_{-m,0} & Q_{-m,1} & \cdots & Q_{-m,m} & r_{-m} \\ \vdots & \vdots & \vdots & \vdots & \vdots & \vdots & \vdots & \vdots \\ Q_{-1,-m} & \cdots & Q_{-1,-1} & Q_{-1,0} & Q_{-1,1} & \cdots & Q_{-1,m} & r_{-1} \\ Q_{0,-m} & \cdots & Q_{0,-1} & Q_{0,0} & Q_{0,1} & \cdots & Q_{0,m} & r_0 \\ Q_{1,-m} & \cdots & Q_{1,-1} & Q_{1,0} & Q_{1,1} & \cdots & Q_{1,m} & r_1 \\ \vdots & \vdots & \vdots & \vdots & \vdots & \vdots & \vdots & \vdots \\ Q_{m,-m} & \cdots & Q_{m,-1} & Q_{m,0} & Q_{m,1} & \cdots & Q_{m,m} & r_m \\ 0 & \cdots & 0 & 0 & 0 & \cdots & 0 & 1 \end{pmatrix}$$

where  $\mathbf{Q}$  is the  $(2m + 1, 2m + 1)$  matrix of transient probabilities,  $\mathbf{0}^\top = (0, 0, \dots, 0)$  and  $\mathbf{r} = \mathbf{1} - \mathbf{Q}\mathbf{1}$ . In addition, the transient probabilities,  $Q_{j,k}$  will be computed as:

$$Q_{j,k} = F_{\text{SN}_t} \left( \frac{H_k + \Delta - (1-\lambda)H_j}{\lambda} \mid n, p_{+1} \right) - F_{\text{SN}_t} \left( \frac{H_k - \Delta - (1-\lambda)H_j}{\lambda} \mid n, p_{+1} \right).$$

where  $F_{\text{SN}_t}(x \mid n, p_{+1})$  is the c.d.f. of  $\text{SN}_t$  as defined in equation (2). Let  $\mathbf{q} = (q_{-m}, \dots, q_0, \dots, q_m)^\top$  be the  $(2m + 1, 1)$  vector of initial probabilities associated with the  $2m + 1$  transient states. In our case, we assume  $\mathbf{q} = (0, \dots, 1, \dots, 0)^\top$  where the

value 1 at the  $m$ -th entry, corresponds to  $Z_0 = E_0(\text{SN}_t) = 0$ . When the number  $2m + 1$  of subintervals is sufficiently large, this approach is supposed to provide an effective method that allows the ARL and SDRL of *continuous* statistics to be accurately evaluated using the following classical formulas from the Markov chains theory (see, for instance [16, 20])

$$\begin{aligned} \text{ARL} &= \mathbf{q}^\top (\mathbf{I} - \mathbf{Q})^{-1} \mathbf{1}, \\ \text{SDRL} &= \sqrt{2\mathbf{q}^\top (\mathbf{I} - \mathbf{Q})^{-2} \mathbf{Q} \mathbf{1} + \text{ARL}(1 - \text{ARL})}. \end{aligned}$$

Generally, in conventional parametric EWMA control charts for monitoring measurement data from a continuous distribution as the number of subintervals (i.e.  $2m + 1$ ) increases the method proposed by Brook and Evans [3] is known to be a reliable approximation of the chart's RL properties. On the other hand, as recent studies have shown (see, for example, Wu et al. in [28]), when the classical method of Brook and Evans [3] is used for the determination of the RL properties of a nonparametric EWMA chart, the ARL values are highly affected by the number of subintervals. Consequently, the standard method of Brook and Evans [3] is not reliable for the computation of the RL properties of a EWMA chart when a discrete statistic is being used for monitoring the time between events. Similarly, Perdakis et al. in [23] verified that the ARL values of a EWMA chart based on the Wilcoxon Signed Rank statistic are highly affected by the number of subintervals.

Following [23, 28], in order to clarify further this point, we present in Table 1 some in- and out-of-control pairs of (ARL, SDRL) values as a function of the number of subintervals  $2m + 1 \in \{51, 61, \dots, 201\}$  for the two-sided SN EWMA chart with parameters  $\lambda = 0.2$ ,  $K = 2.75$ . The (ARL, SDRL) values have been calculated by using the "standard" Markov chain method presented above. The  $(\lambda, K)$  values have been selected for illustrative purposes. In practice, for the EWMA schemes, a general recommendation is to set  $\lambda \approx 0.2$  and  $K \approx 2.7$  (see, for example, [19]). Moreover, the corresponding (ARL, SDRL) values have been estimated via Monte Carlo simulation ( $10^6$  runs) and they are presented in the last row (labelled as "sim") of Table 1. From Table 1, it can be seen that the ARL values of the two-sided SN EWMA chart obtained using the "classical" Markov Chain method presented in [3] are affected by the number of subintervals  $2m + 1$ . In particular, regarding the in-control case, when  $(n, p_{+1}) = (13, 0.5)$  the  $\text{ARL}_0$  values vary from 271.4 to 300.4 while the corresponding simulated  $\text{ARL}_0 = 286.6$ . Similarly, when  $(n, p_{+1}) = (21, 0.5)$  the  $\text{ARL}_0$  values vary from 275.9 to 306.4 while the corresponding simulated  $\text{ARL}_0 = 279.6$ . As a result, practitioners might not be able to find the optimal design parameters of the two-sided SN EWMA chart if the  $\text{ARL}_0$  values are computed through the standard Markov Chain method presented in [3]. Additionally, the same pattern also occurs for the out-of-control scenarios where, for each case, the corresponding  $\text{ARL}_1$  values are not stable. It is also worth stretching that exactly the same pattern occurs for the corresponding SDRL values which clearly depend on the number of subintervals  $2m + 1$ . As a consequence, based on the above findings, we can argue that the use of the classical Markov chain method presented in [3], does not yield reliable results regarding the determination of the chart's in- and out-of-control performances in the case of the two-sided SN EWMA control chart. In order to tackle this problem, in the next Section, a simple methodology originally introduced in [28] will be proposed which not only guarantees robust results for the in- and out-of-control ARL values,

but also allows to find an optimal pair  $(\lambda^*, K^*)$  with corresponding  $ARL_0$  to be *exactly* equal to the desired one (say for instance  $ARL_0 = 370.4$ ).

## 2.2. The “continuousify” approach

In Section 2.1, we emphasized the fact that the number of subintervals  $2m + 1$  affects the ARL values when the standard method of Brook and Evans [3] is used. As a solution to this problem Wu et al. in [28] stated that a combination of the traditional approach of Brook and Evans [3] along with a continuous transformation of the discrete non-parametric statistic (such as the Sign or the Wilcoxon signed ranked statistic), results to steady ARL values and makes their calculation unaffected by the number of subintervals. More specifically, let  $X$  be a discrete random variable defined on the set  $\Psi = \{\psi_1, \psi_2, \dots\}$  with corresponding p.m.f.  $f_X(\psi|\boldsymbol{\theta})$  and  $\boldsymbol{\theta}$  be a vector of parameters. Then, the discrete random variable  $X$  can be represented by a new continuous random variable,  $X^*$ , defined as a mixture of normally distributed random variables  $Y_{\psi_1}^*, Y_{\psi_2}^*, \dots$  where, for each  $\psi \in \Psi$ ,  $Y_{\psi}^*$  follows a normal distribution with mean  $\psi$  and standard deviation  $\sigma$  (i.e.  $Y_{\psi}^* \sim N(\psi, \sigma)$ ). Consequently, the corresponding p.m.f.  $f_{X^*}(x|\boldsymbol{\theta})$  and c.d.f.  $F_{X^*}(x|\boldsymbol{\theta})$  of  $X^*$  will be defined as:

$$f_{X^*}(x|\boldsymbol{\theta}) = \sum_{\psi \in \Psi} f_X(\psi|\boldsymbol{\theta}) f_N(x|\psi, \sigma), \quad (3)$$

$$F_{X^*}(x|\boldsymbol{\theta}) = \sum_{\psi \in \Psi} f_X(\psi|\boldsymbol{\theta}) F_N(x|\psi, \sigma), \quad (4)$$

where  $f_N(x|\psi, \sigma)$  and  $F_N(x|\psi, \sigma)$  are the p.d.f. and c.d.f. of the  $N(\psi, \sigma)$  distribution, respectively, and  $\sigma > 0$  is a fixed parameter known as the “continuousify” parameter. It is worth stretching that the choice of the Normal distribution for defining the p.m.f. and c.d.f. in equations (3) and (4) is just a possible choice among many others. In particular, Perdakis et al. in [23] already tested several symmetrical distributions/kernels (such as Normal, Parabolic, Biweight, Triweight, Cosine) and they concluded that the choice of the distribution has almost *no impact* on the computation of the ARL. Therefore, the practitioner is free to choose the distribution (kernel) of his/her choice as it will not significantly impact the results. For our proposed EWMA control chart based on the Sign statistic, since  $SN_t$  is defined in  $\Psi = \{-n, -n + 2, \dots, n - 2, n\}$ , it can be transformed into a new *continuous* one, based on the Normal Kernel, denoted as  $SN_t^*$  with corresponding p.d.f.  $f_{SN_t^*}(s|n, p_{+1})$  and c.d.f.  $F_{SN_t^*}(s|n, p_{+1})$  defined for  $s \in \mathbb{R}$  as:

$$f_{SN_t^*}(s|n, p_{+1}) = \sum_{\psi \in \Psi} f_{\text{Bin}}\left(\frac{\psi + n}{2} | n, p_{+1}\right) f_N(s|\psi, \sigma),$$

$$F_{SN_t^*}(s|n, p_{+1}) = \sum_{\psi \in \Psi} f_{\text{Bin}}\left(\frac{\psi + n}{2} | n, p_{+1}\right) F_N(s|\psi, \sigma),$$

where  $f_{\text{Bin}}(\dots | n, p_{+1})$  is the p.m.f. of the Binomial distribution with parameters  $n$  and  $p_{+1}$ . Finally, the plotting statistic of the “continuousified” two-sided SN EWMA (denoted as the C-SN EWMA chart) will be computed through the recursive formula as:

$$Z_t^* = \lambda SN_t^* + (1 - \lambda) Z_{t-1}^*, Z_0^* = E_0(SN_t^*). \quad (5)$$

It can be easily proven that the in-control mean  $E_0(\text{SN}_t^*)$  and variance  $V_0(\text{SN}_t^*)$  of  $\text{SN}_t^*$  are equal to:

$$E_0(\text{SN}_t^*) = E_0(\text{SN}_t) = 0, \quad (6)$$

$$V_0(\text{SN}_t^*) = V_0(\text{SN}_t) + \sigma^2 = n + \sigma^2, \quad (7)$$

and, therefore, the control limits  $\text{LCL}^*$  and  $\text{UCL}^*$  of the two-sided C-SN EWMA chart are

$$\text{LCL}^* = -K\sqrt{\frac{(n + \sigma^2)\lambda}{2 - \lambda}}, \quad (8)$$

$$\text{UCL}^* = +K\sqrt{\frac{(n + \sigma^2)\lambda}{2 - \lambda}}. \quad (9)$$

In Table 1, besides the in- and out-of-control pairs of (ARL, SDRL) values of the two-sided SN EWMA chart (computed through the standard method of [3]), the corresponding pairs of (ARL, SDRL) values of the proposed two-sided C-SN EWMA chart (where the “continuousify” method is used) are also reported using the same design parameters  $\lambda = 0.2$ ,  $K = 2.75$ . It should be noted that, in Table 1, even though the value of  $\sigma = 0.2$  is fixed, as it will be explained hereafter through a numerical analysis, the results remain the same regardless the value of  $\sigma$ . Finally, the RL properties of the two-sided C-SN EWMA control chart, are derived through the standard discrete-time Markov chain approach of Brook and Evans [3] presented in Section 2.1 with the only difference that in the computation of the transient probabilities  $Q_{j,k}$  the p.d.f. of  $\text{SN}_t$  is substituted by the p.d.f. of the transformed statistic  $\text{SN}_t^*$ .

Based on the results in Table 1, we can conclude that:

- The in-control ARL values obtained using the standard method of Brook and Evans [3] are affected by the number of subintervals  $2m + 1$ . As it was highlighted in the previous Section, in case when  $(n = 21, p_{+1} = 0.5)$  the  $\text{ARL}_0$  values vary from 275.9 to 306.4 while the corresponding simulated  $\text{ARL}_0 = 279.6$ .
- On the other hand, the use of the “continuousify” method of Wu et al.[28] yields steady and robust results even small values like  $2m + 1 \approx 51$ . More specifically, when  $(n, p_{+1}) = (21, 0.5)$ , the ARL values obtained through “continuousify” method converge to 280.3 quite soon even when  $2m + 1 \approx 51$ . Strictly speaking, only some minor differences in the first decimal place do exist but they are small and will not affect the performance of the chart.
- It is worth stretching that a similar behaviour is also noticed for the corresponding SDRL values. For every case it can be clearly seen that the “continuousify” method yields robust and stable SDRL results when  $2m + 1 \approx 51$ .

Note also that it can be observed that the pairs of (ARL, SDRL) values obtained with the “continuousify” method (see for example the cases when  $2m + 1 = 201$ ), are almost the same or just a bit larger than the ones obtained using simulations which are given in the last line of Table 1.

Regarding the choice of the optimal value of the “continuousify” parameter  $\sigma$ , in Table 2 we present a sensitivity analysis under different combinations of  $n$  and  $p_{+1}$



**Table 1.** Comparison of in- and out-of-control pairs of (ARL,SDRL) values for the two-sided SN EWMA (without “continuousify”) and two-sided C-SN EWMA (with “continuousify” and  $\sigma = 0.2$ ) charts when  $\lambda = 0.2$  and  $K = 2.75$ .

$2m + 1$	$(n = 6, p_{+1} = 0.5)$		$(n = 8, p_{+1} = 0.5)$		$(n = 13, p_{+1} = 0.5)$		$(n = 21, p_{+1} = 0.5)$	
	SN EWMA	C-SN EWMA	SN EWMA	C-SN EWMA	SN EWMA	C-SN EWMA	SN EWMA	C-SN EWMA
51	(299.3,295.1)	(309.3,304.9)	(328.2,323.8)	(293.1,288.8)	(297.1,293)	(287.4,283.2)	(306.4,302.2)	(282.2,278)
61	(311.9,307.5)	(309.8,305.4)	(290,285.6)	(293.6,289.3)	(271.4,267.3)	(287.1,282.9)	(285.5,281.3)	(279.2,275.1)
71	(292.3,287.9)	(310.1,305.7)	(276.8,272.5)	(293.9,289.6)	(280.7,276.5)	(287.4,283.2)	(283.3,279.2)	(279.6,275.4)
81	(312.5,308)	(310.3,305.9)	(309.2,304.8)	(294.1,289.8)	(299.5,295.3)	(287.6,283.4)	(277.9,273.7)	(279.7,275.6)
91	(304.8,300.5)	(310.4,306)	(297.4,293.1)	(294.3,289.9)	(284.7,280.5)	(287.7,283.5)	(281.8,277.6)	(279.9,275.7)
101	(312.5,308)	(310.5,306.1)	(285.9,281.6)	(294.4,290)	(294.5,290.2)	(287.8,283.6)	(301.2,297)	(280,275.8)
111	(310.5,306.2)	(310.6,306.2)	(287.3,283)	(294.4,290.1)	(282.3,278.1)	(287.9,283.7)	(282.8,278.7)	(280,275.9)
121	(309.4,305)	(310.6,306.2)	(291.7,287.4)	(294.5,290.2)	(283.7,279.5)	(288,283.8)	(283.8,279.7)	(280.1,275.9)
131	(315,310.6)	(310.7,306.3)	(284.6,280.2)	(294.5,290.2)	(300.4,296.3)	(288,283.8)	(276.7,272.6)	(280.1,276)
141	(310.6,306.2)	(310.7,306.3)	(291.2,287)	(294.6,290.3)	(286.9,282.7)	(288,283.8)	(279.7,275.6)	(280.2,276)
151	(307.8,303.4)	(310.7,306.3)	(300.2,295.9)	(294.6,290.3)	(281.3,277.1)	(288.1,283.8)	(268.1,264)	(280.3,276.1)
161	(304.3,300)	(310.8,306.4)	(300.1,295.7)	(294.6,290.3)	(291.9,287.7)	(288.1,283.9)	(281.9,277.7)	(280.2,276.1)
171	(305.9,301.5)	(310.8,306.4)	(288,283.7)	(294.7,290.3)	(284.8,280.6)	(288.1,283.9)	(282.6,278.5)	(280.2,276.1)
181	(305.8,301.4)	(310.8,306.4)	(294.3,289.9)	(294.7,290.4)	(287.1,282.8)	(288.1,283.9)	(278.2,274.1)	(280.3,276.1)
191	(309.4,305)	(310.8,306.4)	(295.1,290.7)	(294.7,290.4)	(288,283.8)	(288.1,283.9)	(277.3,273.2)	(280.3,276.1)
201	(304.9,300.5)	(310.8,306.4)	(289.7,285.4)	(294.7,290.4)	(290.8,286.6)	(288.1,283.9)	(275.9,271.7)	(280.3,276.1)
sim	(310.7,304.8)		(293.9,289.2)		(286.6,282.5)		(279.6,274.3)	

$2m + 1$	$(n = 7, p_{+1} = 0.52)$		$(n = 8, p_{+1} = 0.55)$		$(n = 19, p_{+1} = 0.53)$		$(n = 24, p_{+1} = 0.52)$	
	SN EWMA	C-SN EWMA	SN EWMA	C-SN EWMA	SN EWMA	C-SN EWMA	SN EWMA	C-SN EWMA
51	(202.3,197.5)	(225.5,220.7)	(92.3,86.8)	(85.8,80.4)	(91.6,86.4)	(92.8,87.6)	(153.6,148.6)	(143.9,138.9)
61	(219.5,214.9)	(225.8,221.1)	(84.9,79.5)	(85.9,80.4)	(91.3,86.2)	(93.1,87.9)	(145.2,140.2)	(142.6,137.7)
71	(232,227.2)	(226,221.3)	(82.5,77.2)	(85.9,80.5)	(92.3,87.1)	(93.2,88)	(144.1,139.1)	(142.7,137.8)
81	(229.6,224.9)	(226.2,221.4)	(88.7,83.2)	(85.9,80.5)	(90.84,8)	(93.2,88)	(141.8,136.9)	(142.8,137.8)
91	(226.6,221.9)	(226.3,221.5)	(86.3,80.8)	(85.9,80.5)	(92.4,87.1)	(93.2,88)	(143.4,138.4)	(142.8,137.9)
101	(230,225.2)	(226.4,221.6)	(83.8,78.4)	(85.9,80.5)	(94.8,89.6)	(93.3,88)	(151.3,146.2)	(142.9,137.9)
111	(227.9,223.2)	(226.4,221.6)	(83.8,78.4)	(86,80.5)	(96.2,91)	(93.3,88)	(143.8,138.8)	(142.9,137.9)
121	(217.9,213.2)	(226.5,221.7)	(85.1,79.7)	(86,80.5)	(92.9,87.7)	(93.3,88.1)	(144.2,139.2)	(142.9,137.9)
131	(227.4,222.6)	(226.5,221.7)	(83.5,78.1)	(86,80.5)	(92.7,87.5)	(93.3,88.1)	(141.4,136.4)	(142.9,137.9)
141	(228.5,223.8)	(226.5,221.7)	(84.9,79.5)	(86,80.5)	(93.7,88.5)	(93.3,88.1)	(142.8,137.8)	(142.9,137.9)
151	(230.2,225.5)	(226.5,221.8)	(86.7,81.3)	(86,80.6)	(92.8,87.6)	(93.3,88.1)	(137.8,132.9)	(142.9,138)
161	(225.5,220.7)	(226.5,221.8)	(86.5,81.1)	(86,80.6)	(94.3,89.1)	(93.3,88.1)	(143.6,138.6)	(142.9,138)
171	(226.1,221.4)	(226.6,221.8)	(84.2,78.8)	(86,80.6)	(93.8,88.5)	(93.3,88.1)	(143.9,138.9)	(143,138)
181	(227.5,222.7)	(226.6,221.8)	(85.5,80.1)	(86,80.6)	(92.7,87.5)	(93.3,88.1)	(142,137)	(143,138)
191	(225.8,221.1)	(226.6,221.8)	(85.6,80.2)	(86,80.6)	(92.5,87.2)	(93.3,88.1)	(141.5,136.5)	(143,138)
201	(226.9,222.1)	(226.6,221.8)	(84.4,79)	(86,80.6)	(94.1,88.8)	(93.3,88.1)	(141.1,136.1)	(143,138)
sim	(225.8,220.7)		(85.6,80.1)		(92.9,87.6)		(143,137.8)	

for  $\lambda = 0.2$ ,  $K = 2.75$ , and  $\sigma \in \{0.1, 0.15, \dots, 0.3\}$ . Based on these results, it can be clearly concluded that the ARL values obtained for the two-sided C-SN EWMA chart are not only very stable, even for small values of  $2m + 1 \approx 51$ , but also they are not seriously affected by the value of the “continuousify” parameter  $\sigma$  with only some minor differences occurring in the first decimal place. As a consequence, as long as  $\sigma$  is neither too small nor too large, the results are not affected by its value. Therefore, for the value of the “continuousify” parameter  $\sigma = 0.2$  can be considered in the rest of the paper as a reasonable choice.

Finally, the results of a numerical study for the performance of the two-sided C-SN EWMA control chart are presented. The desired in-control ARL value is set equal to 370.4 and no head-start feature has been used (i.e  $Z_0^* = 0$ ). In Table 3, the optimal pairs of the design parameters ( $\lambda^*, K^*$ ) are provided for different shifts ( $p_{+1}$ ) and sample sizes ( $n$ ) along with the corresponding  $ARL_1$  values setting the number of subintervals equal to  $2m + 1 = 201$ . Since, we are investigating shifts in the process median (i.e when the process is in-control we have  $p_{+1} = 0.5$ ) an out-of-control value of  $p_{+1}$  close to 0.5 corresponds to a “small” shift from  $\theta_0$  to  $\theta_1$ . On the other hand, an out-of-control value of  $p_{+1}$  close 0 or 1 corresponds to a “large” shift from  $\theta_0$  to  $\theta_1$ . Note that, due to the symmetry of the distribution (assuming  $\theta_0$  as the in-control median) it is only necessary to investigate  $p_{+1} \in (0.5, 1)$  since the results are the same for  $p_{+1} \in (0, 0.5)$ . For the determination of the optimal pair ( $\lambda^*, K^*$ ) for the two-sided C-SN EWMA chart, the

**Table 2.** ARL values of the two-sided C-SN EWMA chart for  $\lambda = 0.2$ ,  $K = 2.75$  and for fixed values of  $\sigma = \{0.1, 0.15, \dots, 0.3\}$  and different combinations of  $(n, p_{+1})$ .

$2m + 1$	$(n, p_1) = (7, 0.5)$					$(n, p_1) = (13, 0.5)$					$(n, p_1) = (15, 0.5)$				
	$\sigma$					$\sigma$					$\sigma$				
	0.1	0.15	0.2	0.25	0.3	0.1	0.15	0.2	0.25	0.3	0.1	0.15	0.2	0.25	0.3
51	295.7	297.4	297.7	297.8	297.8	294.1	289.5	287.4	286.7	286.4	281.4	282.1	282.4	282.6	282.8
61	298.5	298.3	298.3	298.4	298.4	286.5	287.0	287.1	287.0	286.9	283.8	283.2	283.1	283.2	283.3
71	298.8	298.6	298.7	298.7	298.7	286.9	287.4	287.4	287.3	287.1	279.2	282.4	283.3	283.5	283.6
81	298.8	298.9	298.9	299.0	298.9	289.0	287.8	287.6	287.5	287.3	283.4	283.5	283.6	283.7	283.8
91	299.0	299.0	299.1	299.1	299.1	287.1	287.8	287.7	287.6	287.4	283.3	283.6	283.7	283.8	283.9
101	299.1	299.1	299.2	299.2	299.2	287.9	287.9	287.8	287.7	287.5	284.4	283.7	283.8	283.9	284.0
111	299.2	299.2	299.3	299.3	299.3	288.0	287.9	287.9	287.8	287.6	283.8	283.8	283.9	284.0	284.1
121	299.2	299.3	299.4	299.4	299.4	287.9	288.0	287.9	287.8	287.6	283.8	283.8	283.9	284.0	284.1
131	299.3	299.4	299.4	299.4	299.4	288.1	288.1	288.0	287.9	287.7	283.8	283.9	284.0	284.1	284.2
141	299.3	299.4	299.4	299.5	299.4	288.1	288.1	288.0	287.9	287.7	283.9	283.9	284.0	284.1	284.2
151	299.4	299.4	299.5	299.5	299.5	288.1	288.1	288.1	287.9	287.7	283.9	283.9	284.0	284.1	284.2
161	299.4	299.4	299.5	299.5	299.5	288.1	288.1	288.1	287.9	287.7	283.9	284.0	284.1	284.2	284.2
171	299.4	299.5	299.5	299.6	299.5	288.1	288.1	288.1	287.9	287.8	283.9	284.0	284.1	284.2	284.3
181	299.4	299.5	299.5	299.6	299.5	288.2	288.2	288.1	288.0	287.8	283.9	284.0	284.1	284.2	284.3
191	299.5	299.5	299.6	299.6	299.6	288.2	288.2	288.1	288.0	287.8	283.9	284.0	284.1	284.2	284.3
201	299.5	299.5	299.6	299.6	299.6	288.2	288.2	288.1	288.0	287.8	283.9	284.0	284.1	284.2	284.3
$g$	$(n, p_1) = (18, 0.53)$					$(n, p_1) = (22, 0.55)$					$(n, p_1) = (25, 0.6)$				
	$\sigma$					$\sigma$					$\sigma$				
	0.1	0.15	0.2	0.25	0.3	0.1	0.15	0.2	0.25	0.3	0.1	0.15	0.2	0.25	0.3
51	97.7	97.7	97.7	97.7	97.7	35.8	35.7	35.7	35.7	35.8	9.1	9.1	9.1	9.1	9.1
61	99.7	98.5	97.9	97.8	97.8	35.6	35.7	35.7	35.7	35.8	9.1	9.1	9.1	9.1	9.1
71	97.8	97.8	97.7	97.8	97.8	35.5	35.6	35.7	35.7	35.8	9.1	9.1	9.1	9.1	9.1
81	97.6	97.7	97.8	97.8	97.8	35.6	35.7	35.7	35.7	35.8	9.1	9.1	9.1	9.1	9.1
91	97.9	97.8	97.8	97.8	97.8	35.6	35.7	35.7	35.7	35.8	9.1	9.1	9.1	9.1	9.1
101	97.8	97.8	97.8	97.8	97.8	35.6	35.7	35.7	35.7	35.8	9.1	9.1	9.1	9.1	9.1
111	97.7	97.8	97.8	97.8	97.8	35.6	35.7	35.7	35.7	35.8	9.1	9.1	9.1	9.1	9.1
121	97.8	97.8	97.8	97.8	97.8	35.7	35.7	35.7	35.7	35.8	9.1	9.1	9.1	9.1	9.1
131	97.8	97.8	97.8	97.8	97.8	35.7	35.7	35.7	35.7	35.8	9.1	9.1	9.1	9.1	9.1
141	97.8	97.8	97.8	97.8	97.8	35.7	35.7	35.7	35.7	35.8	9.1	9.1	9.1	9.1	9.1
151	97.8	97.8	97.8	97.8	97.8	35.7	35.7	35.7	35.7	35.8	9.1	9.1	9.1	9.1	9.1
161	97.8	97.8	97.8	97.8	97.8	35.7	35.7	35.7	35.7	35.8	9.1	9.1	9.1	9.1	9.1
171	97.8	97.8	97.8	97.8	97.8	35.7	35.7	35.7	35.7	35.8	9.1	9.1	9.1	9.1	9.1
181	97.8	97.8	97.8	97.8	97.8	35.7	35.7	35.7	35.7	35.8	9.1	9.1	9.1	9.1	9.1
191	97.8	97.8	97.8	97.8	97.8	35.7	35.7	35.7	35.7	35.8	9.1	9.1	9.1	9.1	9.1
201	97.8	97.8	97.8	97.8	97.8	35.7	35.7	35.7	35.7	35.8	9.1	9.1	9.1	9.1	9.1

following procedure was utilised: Find out the optimal pair  $(\lambda^*, K^*)$  such that for a fixed value of sample size  $n$ , we have  $ARL(n, \lambda^*, K^*, p_{+1} = 0.5) = 370.4$  and, for a fixed value of  $p_{+1} \in \{0.55, 0.6, \dots, 0.95\}$ ,  $ARL(n, \lambda^*, K^*, p_{+1})$  is the smallest out-of-control ARL. It is worth mentioning that (see, for example, [5]), for the two-sided Shewhart chart based on the Sign statistic it is impossible to obtain an in-control  $ARL_0 \approx 370$  for small values of the sample size  $n$  (e.g. for  $n \in \{2, 3, \dots, 10\}$ ). Additionally, for small values of  $\lambda$  singularity problems might occur during the optimization procedure. On the contrary, based on the results presented in Table 3, it can be observed that, in the proposed C-SN EWMA scheme, we are able to find an optimal pair of parameters  $(\lambda^*, K^*)$  giving an  $ARL_0$  exactly equal to 370.4 even for  $n = 2$  and  $\lambda \approx 0.02$ . For the above computations, the Markov chain method presented in Section 2.1 was used and all the calculations were performed in R. For any combination of  $\lambda$  and  $K$  and for given values  $n$  and  $p_{+1}$ , by using a computer with Intel(R) Core(TM) i7-7500U CPU, it takes about 0.5 seconds to get the values (ARL, SDRL) for the two-sided C-SN EWMA chart using for  $2m + 1 \approx 101$ . On the other hand, in order to obtain a relatively robust result with the standard method of Brook and Evans, the number of subintervals should be at least  $2m + 1 \approx 501$  (see, [14]). The corresponding time for these computations is 1.42 seconds.

### 3. Distribution of the Sign statistic when ties are present

Generally, the smooth operation of a control chart during the on-line process monitoring, besides it's theoretical optimal design, relies on the sample's values accuracy collected at each sampling point  $t$ . However in practice, due to the measurement

**Table 3.** Optimal combinations of  $(\lambda^*, K^*)$  for the two-sided C-SN EWMA chart along with the corresponding  $ARL_1$  values.

$n$	$P_{+1}$						
	0.55	0.60	0.65	0.70	0.80	0.85	0.9
2	(0.02,2.138,135.61)	(0.02,2.138,57.65)	(0.04,2.41,33.49)	(0.06,2.54,22.2)	(0.12,2.693,11.97)	(0.16,2.719,9.3)	(0.195,2.72,7.43)
3	(0.02,2.14,106.54)	(0.03,2.304,44.087)	(0.055,2.509,25.13)	(0.085,2.62,16.48)	(0.15,2.737,8.72)	(0.19,2.769,6.81)	(0.31,2.757,5.38)
4	(0.02,2.138,89.04)	(0.035,2.363,36.21)	(0.065,2.57,20.38)	(0.1,2.682,13.26)	(0.185,2.775,7.01)	(0.215,2.783,5.46)	(0.33,2.798,4.32)
5	(0.02,2.138,77.25)	(0.04,2.407,31.03)	(0.08,2.621,17.3)	(0.12,2.726,11.18)	(0.215,2.814,5.89)	(0.345,2.815,4.59)	(0.455,2.799,3.46)
6	(0.02,2.137,68.74)	(0.05,2.489,27.27)	(0.09,2.661,15.11)	(0.135,2.746,9.76)	(0.27,2.844,5.06)	(0.295,2.848,3.91)	(0.315,2.849,3.13)
7	(0.02,2.137,62.29)	(0.055,2.513,24.44)	(0.1,2.69,13.46)	(0.145,2.771,8.67)	(0.33,2.857,4.53)	(0.37,2.861,3.48)	(0.38,2.862,2.81)
8	(0.02,2.137,57.2)	(0.06,2.548,22.2)	(0.11,2.709,12.19)	(0.175,2.805,7.82)	(0.285,2.863,4.09)	(0.36,2.866,3.18)	(0.4,2.865,2.56)
9	(0.025,2.229,53.03)	(0.065,2.572,20.38)	(0.12,2.736,11.15)	(0.18,2.811,7.16)	(0.345,2.881,3.72)	(0.38,2.882,2.91)	(0.715,2.838,2.19)
10	(0.025,2.231,49.47)	(0.07,2.594,18.88)	(0.135,2.76,10.29)	(0.195,2.83,6.6)	(0.375,2.887,3.45)	(0.66,2.866,2.65)	(0.67,2.865,1.94)
11	(0.025,2.228,46.48)	(0.075,2.616,17.61)	(0.135,2.763,9.58)	(0.205,2.835,6.14)	(0.525,2.894,3.22)	(0.545,2.893,2.4)	(0.565,2.891,1.87)
12	(0.03,2.303,43.85)	(0.08,2.632,16.53)	(0.145,2.781,8.96)	(0.23,2.856,5.73)	(0.47,2.902,2.98)	(0.485,2.9,2.3)	(0.505,2.898,1.84)
13	(0.03,2.3,41.57)	(0.085,2.652,15.57)	(0.165,2.802,8.44)	(0.24,2.866,5.39)	(0.435,2.908,2.8)	(0.745,2.889,2.05)	(0.77,2.885,1.5)
14	(0.03,2.303,39.55)	(0.095,2.68,14.74)	(0.16,2.802,7.98)	(0.26,2.873,5.1)	(0.595,2.91,2.65)	(0.625,2.907,1.95)	(0.645,2.905,1.49)
15	(0.035,2.36,37.73)	(0.095,2.683,14)	(0.17,2.811,7.57)	(0.25,2.874,4.84)	(0.535,2.915,2.49)	(0.555,2.914,1.89)	(0.56,2.914,1.49)
16	(0.035,2.362,36.1)	(0.1,2.696,13.35)	(0.18,2.824,7.2)	(0.27,2.884,4.6)	(0.48,2.921,2.38)	(0.78,2.91,1.77)	(0.8,2.91,1.33)
17	(0.035,2.361,34.65)	(0.105,2.708,12.76)	(0.19,2.836,6.87)	(0.28,2.888,4.4)	(0.65,2.921,2.25)	(0.69,2.918,1.64)	(0.71,2.916,1.26)
18	(0.04,2.411,33.3)	(0.11,2.721,12.22)	(0.195,2.838,6.59)	(0.285,2.894,4.21)	(0.59,2.926,2.13)	(0.59,2.926,1.62)	(0.95,2.874,1.27)
19	(0.04,2.411,32.07)	(0.115,2.73,11.74)	(0.2,2.846,6.32)	(0.34,2.913,4.03)	(0.51,2.931,2.09)	(0.8,2.924,1.56)	(0.815,2.925,1.21)
20	(0.04,2.411,30.96)	(0.12,2.743,11.29)	(0.22,2.861,6.07)	(0.305,2.903,3.89)	(0.69,2.93,1.94)	(0.72,2.928,1.43)	(0.73,2.928,1.14)

system resolution, the real values  $X_{t,j}$  are not directly observed. Instead, a measured value  $X'_{t,j} \neq X_{t,j}$  is obtained introducing a rounding-off error which results in a discretization of the observed measures. Note that, even if the sample's true distribution is continuous, the presence of rounding-off errors might result in "ties" between the real values  $X_{t,j}$  and the in-control value  $\theta_0$  of the median.

A well known linear measurement error model to account for three well-known sources of error is (see [17]):

$$X'_{t,j} = \left\lfloor \frac{A + BX_{t,j} + \varepsilon_{t,j}}{\rho} + \frac{1}{2} \right\rfloor \rho, \quad (10)$$

where the constants  $(A, B)$  are related with the bias- linearity error, the noise  $\varepsilon_{t,j}$  (r.v.) accounts for the precision error and  $\rho$  is a parameter quantifying the device resolution, which introduces a rounding-off error. More specifically, if  $\rho$  is the resolution of the measurement system then  $X'_{t,j} = x$  if  $X_{t,j} \in (x - \frac{\rho}{2}, x + \frac{\rho}{2})$ . For instance, if  $\rho = 0.2$  and  $\theta_0 = 100$  then possible measured values  $X'_{t,j}$  are  $\{\dots 99.6, 99.8, 100, 100.2, 100.4, \dots\}$  and, if the real value is  $X_{t,j} = 100.038$ , then the measured observation is  $X'_{t,j} = 100$ . As a consequence, a tie is generated. In general, the rounding-off error introduced by the device resolution in the measurement of the true value of a quality characteristic, results in a discretization of the observed quality characteristic and, in case of continuous measurements, the probability of having ties is therefore increased. In this work, we will investigate the effect of the tool resolution by maintaining the assumption of a perfect tool calibration,  $(A, B) = (0, 1)$  and overlook the precision error. As a consequence, the error model given in (10) will simply be defined as:

$$X'_{t,j} = \left\lfloor \frac{X_{t,j}}{\rho} + \frac{1}{2} \right\rfloor \rho, \quad (11)$$

In Section 2, it was stated that when  $X$  is a continuous random variable, regardless

the value of  $\theta$ , we always have  $p_0 = P(X_{t,j} = \theta_0) = 0$ . However, due to the occurrence of tied observations caused by the rounding-off errors of the measurement system, the statistic  $S_{t,j}$  presented in Section 2 is no longer defined on  $\{-1, 1\}$  but rather on  $\{-1, 0, 1\}$ . As a consequence,  $S_{t,j} = \text{sign}(X_{t,j} - \theta_0)$  has to be replaced by  $S_{t,j} = \text{sign}(X'_{t,j} - \theta_0)$  and the vector of probabilities  $\mathbf{p} = (p_{-1}, p_0, p_{+1})$  must be redefined as:

$$p_{-1} = P(X'_{t,j} < \theta_0) = P\left(X_{t,j} \leq \theta_0 - \frac{\rho}{2}\right) = F_X\left(\theta_0 - \frac{\rho}{2}|\theta\right),$$

$$\begin{aligned} p_0 &= P(X'_{t,j} = \theta_0) = P\left(\theta_0 - \frac{\rho}{2} < X_{t,j} \leq \theta_0 + \frac{\rho}{2}\right) \\ &= F_X\left(\theta_0 + \frac{\rho}{2}|\theta\right) - F_X\left(\theta_0 - \frac{\rho}{2}|\theta\right), \end{aligned}$$

$$p_{+1} = P(X'_{t,j} > \theta_0) = P\left(X_{t,j} > \theta_0 + \frac{\rho}{2}\right) = 1 - F_X\left(\theta_0 + \frac{\rho}{2}|\theta\right).$$

Without loss of generality, let us assume that the process shift can be expressed in terms of the standardized distribution shift of magnitude  $\delta$ , as  $\theta_1 = \theta_0 + \delta\omega$ . Also, we assume that  $F_X(x|\theta)$  belongs to a location-scale family of distributions which can be rewritten as  $F_X(x|\theta) = F_Z\left(\frac{x-\theta}{\omega}\right)$  where  $\omega$  is the standard deviation of  $X$ . If we define the quantity  $\kappa = \frac{\rho}{\omega}$  as the standardized resolution, the vector of probabilities  $\mathbf{p} = (p_{-1}, p_0, p_{+1})$  can be rewritten as:

$$\begin{aligned} p_{-1} &= F_Z\left(-\frac{\kappa}{2} - \delta\right), \\ p_0 &= F_Z\left(\frac{\kappa}{2} - \delta\right) - F_Z\left(-\frac{\kappa}{2} - \delta\right), \\ p_{+1} &= 1 - F_Z\left(\frac{\kappa}{2} - \delta\right). \end{aligned} \tag{12}$$

which simplify to

$$\begin{aligned} p_{-1} &= F_Z\left(-\frac{\kappa}{2}\right), \\ p_0 &= F_Z\left(\frac{\kappa}{2}\right) - F_Z\left(-\frac{\kappa}{2}\right), \\ p_{+1} &= 1 - F_Z\left(\frac{\kappa}{2}\right). \end{aligned}$$

when the process is in-control (i.e.  $\delta = 0$ ). It can be clearly concluded that, the variable  $\text{SN}_t$  is no longer defined on  $\{-n, -n+2, \dots, n-2, n\}$  but it is rather defined on  $\{-n, -n+1, \dots, n-1, n\}$  and the p.m.f. of  $\text{SN}_t$  cannot be computed through the binomial distribution as in (2). The p.m.f.  $f_{\text{SN}_t}(s|n, \mathbf{p})$  of  $\text{SN}_t$  in presence of ties has

already been derived by Castagliola et al. in [4] and is equal to

$$f_{\text{SN}_t}(s|n, \mathbf{p}) = \sum_{i=\max(0, -s)}^{\lfloor \frac{n-s}{2} \rfloor} \binom{n}{i} \binom{n-i}{s+i} p_{-1}^i p_0^{n-s-2i} p_{+1}^{s+i}. \quad (13)$$

Finally, regarding the computation of the distribution of the transformed variable,  $\text{SN}_t^*$ , when ties are present it will be computed as:

$$f_{\text{SN}_t^*}(s|n, \mathbf{p}) = \sum_{\psi \in \Psi} f_{\text{SN}_t}(\psi|n, \mathbf{p}) f_{\text{N}}(s|\psi, \sigma),$$

$$F_{\text{SN}_t^*}(s|n, \mathbf{p}) = \sum_{\psi \in \Psi} f_{\text{SN}_t}(\psi|n, \mathbf{p}) F_{\text{N}}(s|\psi, \sigma),$$

where  $f_{\text{SN}_t}(\psi|n, \mathbf{p})$  is the p.m.f. of  $\text{SN}_t$  when ties are present defined in (13) with parameters  $n$  and the vector of probabilities  $\mathbf{p} = (p_{-1}, p_0, p_{+1})$  presented in (12). Note that, when ties are present, the two-sided C-SN EWMA chart is no longer distribution-free since the in-control distribution of  $\text{SN}_t$  depends on  $F_X(x|\theta)$  through the vector of probabilities  $\mathbf{p} = (p_{-1}, p_0, p_{+1})$ . Additionally, the domain  $\Psi$  depends on the value of  $\kappa$ . More specifically, when  $\kappa = 0$ ,  $\Psi \in \{-n, -n+2, \dots, n-2, n\}$  and for  $\kappa > 0$ ,  $\Psi \in \{-n, -n+1, \dots, n-1, n\}$ .

#### 4. Effect of the measurement system resolution

In this Section, we will investigate the effect of the measurement system resolution and the related probability to have tied observations under different design scenarios. As it was previously stated, in cases where ties are present, the proposed C-SN EWMA chart, is no longer distribution free. In order to investigate the chart's RL properties, following a semi-parametric design already suggested in [4], we will examine the in- and out-of-control robustness of the two-sided C-SN EWMA chart under a benchmark of 17 Johnson's type distributions covering a wide range of skewness  $\gamma_3$  and kurtosis  $\gamma_4$ . By definition, a Johnson's-type distribution depends on four parameters  $a, b > 0$ ,  $c$  and  $d > 0$  and it is defined as:

- bounded on  $[c, c+d]$  (denoted as B in Table 4) with  $F_Z(x)$  equal to:

$$F_Z(x) = F_{\text{N}}\left(a + b \ln\left(\frac{x-c}{c+d-x}\right)\right),$$

- unbounded on  $(-\infty, \infty)$  (denoted as U in Table 4) with  $F_Z(x)$  equal to:

$$F_Z(x) = F_{\text{N}}\left(a + b \sinh^{-1}\left(\frac{x-c}{d}\right)\right).$$

The vector of parameters  $a, b, c, d$  for the 17 Johnson's type distributions (Table 4), are such that the conditions  $\text{med}(Z) = 0$  (for the median) and  $\sigma(Z) = 1$  (for the standard-deviation) are fulfilled. In terms of skewness ( $\gamma_3$ ) and kurtosis ( $\gamma_4$ ), cases 1-6 correspond (without being exactly identical) to some well known symmetric

**Table 4.** Benchmark of 17 Johnson's type distributions.

case	$\gamma_3$	$\gamma_4$	type	$a$	$b$	$c$	$d$
1	0	-1.2	B	0	0.64646	-1.81530	3.63060
2	0	-0.6	B	0	1.39830	-3.10970	6.21950
3	0	0	U	0	100	0	100
4	0	1	U	0	2.3212	0	2.10940
5	0	3	U	0	1.6104	0	1.31180
6	0	6	U	0	1.3493	0	1
7	2	4.3	B	1.7464	0.69076	-0.48932	6.6213
8	2	6.1	B	3.3279	1.227	-1.0016	16.088
9	2	7.9	U	-4.85600	1.8044	-1.41900	0.19332
10	2	10.8	U	-1.0444	1.432	-0.65538	0.82361
11	2	16.7	U	-0.52977	1.2093	-0.33154	0.73314
12	2	25.5	U	-0.34371	1.0892	-0.2023	0.63054
13	5	52.6	B	5.2193	0.98134	-0.47316	97.043
14	5	65.3	U	-4.01870	1.0864	-0.56652	0.02806
15	5	86	U	-0.75701	0.98744	-0.32033	0.37954
16	5	128.7	U	-0.43187	0.90797	-0.18538	0.37543
17	5	192.1	U	-0.29868	0.85558	-0.12122	0.34029

distributions. More specifically, case 1 corresponds to the uniform distribution, case 2 corresponds to the triangular distribution, case 3 corresponds to the normal distribution (setting  $b = d = 100$ ) and cases 4-6 correspond to the Student  $t$  distribution with 10, 6 and 5 degrees of freedom, respectively. Finally, cases 7-17 cover a large variety of asymmetric distributions with various values for the skewness  $\gamma_3 > 0$  and kurtosis  $\gamma_4 > 0$ . A graphical representation of all these Johnson's distribution can be found in page 116 in [4].

In this work, we aim to present a suitable procedure to reduce or, ideally, eliminate the effect of the rounding-off error providing an efficient design of a nonparametric Sign EWMA chart capable of handling scenarios where tied observations occur during the process monitoring. The rest of this Section is organised as follows. For the 17 Johnson's type distributions presented in Table 4, the ARL values of the two-sided C-SN EWMA control chart will be presented for shifts  $\delta \in \{-0.5, -0.2, -0.1, 0, 0.1, 0.2, 0.5\}$  and for standardized resolution  $\kappa = 0$  (without ties) and  $\kappa \in \{0.05, 0.1, 0.2\}$  (with ties) using two different strategies. More specifically, in Section 4.1 the same control limits ( $UCL^*, LCL^*$ ) will be used, for the 17 Johnson's type distributions. In Section 4.2 a Bernoulli trial-based approach will be investigated where tied observations will be equally treated as negative or positive differences. For each approach and a fixed value of  $n = 20$ , two optimal pairs  $(\lambda^*, K^*)$  listed in Table 3 will be investigated:

- The first optimal pair is  $(\lambda^* = 0.12, K^* = 2.743)$ . This one corresponds to the optimal pair  $(\lambda^*, K^*)$  for detecting a shift corresponding to a small value  $p_{+1} = 0.6$  for  $n = 20$ . The value  $p_{+1} = 0.6$  is considered as a small shift in the in-control process median.
- The second optimal pair is  $(\lambda^* = 0.72, K^* = 2.928)$ . This one corresponds to optimal pair  $(\lambda^*, K^*)$  for detecting a shift corresponding to a moderate to large value  $p_{+1} = 0.85$  for  $n = 20$ . The value  $p_{+1} = 0.8$  corresponds to a moderate shift in the in-control process median.

#### 4.1. Run length properties of the C-SN EWMA using the traditional control limits

In this section we will examine the RL properties of the two-sided C-SN EWMA chart under tied scenarios using the charting statistic defined in equation (5) and the fixed control limits as defined in equations (8) and (9). Regarding the computation of the

control limits, the in-control mean,  $E_0(\text{SN}_t^*)$  and variance,  $V_0(\text{SN}_t^*)$  of  $\text{SN}_t^*$  will be the same for all the cases regardless the underlying distribution as defined in (6) and (7). From the results in Table 5 (top) we can conclude the following:

- For  $\kappa = 0$  the in-control values of ARL are steady and *exactly* equal to 370.4 (as expected). Note that this is an advantage of our proposed scheme since, regardless the sample size, it can be designed giving a corresponding in-control ARL value, to be exactly equal to the predefined value of  $\text{ARL}_0$ . On the other hand, for  $\kappa > 0$ , even for small values of  $\kappa$ , the in-control ARL values are different. For example when  $(p_{+1}, \lambda, K) = (0.6, 0.12, 2.743)$  and  $\kappa = 0.05$  we have  $\text{ARL}_0 = 391.1$  for case 1 and  $\text{ARL}_0 = 432.2$  for case 15. In addition, for heavy tailed distributions ( i.e for large values of  $\gamma_4$ ) the  $\text{ARL}_0$  values become larger (see for example the last four cases).
- For the first 6 symmetric cases the corresponding out-of-control values are the same for shifts  $\delta$  and  $-\delta$  regardless the value of  $\kappa$ . On the other hand, for the asymmetric cases, negative shifts,  $\delta$  give larger  $\text{ARL}_1$  values than positive ones. For example, in case 10, when  $(p_{+1}, \lambda, K) = (0.6, 0.12, 2.743)$  and  $\kappa = 0.2$  for  $\delta = -0.1$  we have  $\text{ARL}_1 = 37.7$  and for  $\delta = 0.1$  we have  $\text{ARL}_1 = 30.6$ .
- Regardless the type of distribution, as  $\kappa$  increases the out-of-control  $\text{ARL}_1$  values are becoming larger. For instance, for  $\delta = 0.1$  and  $(p_{+1}, \lambda, K) = (0.85, 0.72, 2.928)$  we have  $\text{ARL}_1 = 131.7$  for  $\kappa = 0$ ,  $\text{ARL}_1 = 143.4$  for  $\kappa = 0.05$ ,  $\text{ARL}_1 = 157.4$  for  $\kappa = 0.1$  and  $\text{ARL}_1 = 193.9$  for  $\kappa = 0.2$ .

#### 4.2. Run length properties of the C-SN EWMA under the “flip a coin strategy”

As it has been proposed by Castagliola et al. in [4], an efficient strategy to handle ties in the design of a Sign chart is the “flip a coin” strategy in which the probability  $p_0$  is equally allocated on both sides for values  $S_{t,j} = +1$  and  $S_{t,j} = -1$ . More specifically, for each value  $S_{t,j} = 0$  it is proposed the transformation  $S_{t,j} = 2\Delta_{t,j} - 1$  where  $\Delta_{t,j} \sim \text{Ber}(0.5)$  is a Bernoulli random variable of parameter 0.5. As a consequence, applying this strategy is equivalent to consider the two-sided C-SN EWMA control chart in the “without ties” case with the following new probabilities:

$$\begin{aligned} p'_{-1} &= p_{-1} + \frac{p_0}{2}, \\ p'_0 &= 0, \\ p'_{+1} &= p_{+1} + \frac{p_0}{2}. \end{aligned}$$

In Table 6, the in-control ( $\delta = 0$ ) vectors of probabilities  $\mathbf{p}' = (p'_{-1}, p'_0, p'_{+1})$  for the 17 distributions are reported for different values of  $\kappa$ . We can conclude that when  $\kappa = 0$ , as expected, we always have  $p'_0 = 0, p'_{+1} = p'_{-1} = 0.5$  no matter the considered distribution. Moreover, for the *symmetric* cases 1 – 6, (when  $\kappa > 0$ ) we always have  $p'_{+1} = p'_{-1} = 0.5$  This is also an expected result. Finally, for the *asymmetric* cases, even though  $p'_{+1}$  differs from  $p'_{-1}$  all the  $p'_{+1}$  values remain really close to 0.5, since  $|p'_{+1} - 0.5| < 0.01$  for the cases 7-17. Next, using the new  $p'_{-1}, p'_{+1}$  probabilities, we evaluated the performance of the C-SN EWMA chart. Based on the results presented

**Table 5.** ARL values when  $n = 20$  for  $(p_{+1}, \lambda, K) = (0.6, 0.12, 2.743)$  and  $(p_{+1}, \lambda, K) = (0.85, 0.72, 2.928)$  with(top) and without(bottom) the “flip a coin” strategy.

		Without the “flip a coin” strategy																											
		$(p_{+1}, \lambda, K) = (0.6, 0.12, 2.743)$																											
		$\kappa = 0$							$\kappa = 0.05$							$\kappa = 0.1$							$\kappa = 0.2$						
		$\delta$							$\delta$							$\delta$							$\delta$						
case		-0.5	-0.2	-0.1	0	0.1	0.2	0.5	-0.5	-0.2	-0.1	0	0.1	0.2	0.5	-0.5	-0.2	-0.1	0	0.1	0.2	0.5	-0.5	-0.2	-0.1	0	0.1	0.2	0.5
1	6.8	28.6	93.5	370.4	93.5	28.6	6.8	6.9	28.8	95.6	391.1	95.6	28.8	6.9	6.9	29.0	97.8	413.4	97.8	29.0	6.9	6.8	29.5	102.3	464.0	102.3	29.5	6.8	
2	5.3	19.3	64.3	370.4	64.2	19.3	5.3	5.3	19.4	65.7	396.8	65.5	19.4	5.3	5.3	19.5	67.1	425.9	67.0	19.5	5.3	5.3	19.8	70.5	494.0	70.3	19.8	5.3	
3	4.7	16.3	53.6	370.4	53.6	16.3	4.7	4.7	16.3	54.7	399.9	54.7	16.3	4.7	4.7	16.4	55.9	432.8	55.9	16.4	4.7	4.8	16.7	58.8	511.4	58.8	16.7	4.8	
4	4.3	14.0	45.4	370.4	45.4	14.0	4.3	4.3	14.1	46.3	403.1	46.3	14.1	4.3	4.3	14.1	47.3	439.9	47.3	14.1	4.3	4.3	14.4	49.7	529.6	49.7	14.4	4.3	
5	3.9	11.9	37.5	370.4	37.5	11.9	3.9	3.9	11.9	38.2	407.1	38.2	11.9	3.9	3.9	12.0	39.0	449.0	39.0	12.0	3.9	4.0	12.2	41.1	553.9	41.1	12.2	4.0	
6	3.6	10.4	31.8	370.4	31.8	10.4	3.6	3.6	10.4	32.3	411.0	32.3	10.4	3.6	3.6	10.5	33.0	458.1	33.0	10.5	3.6	3.7	10.7	34.8	578.7	34.8	10.7	3.7	
7	4.3	10.9	29.8	370.4	21.5	6.4	2.0	4.3	11.0	30.5	416.5	21.5	6.4	2.0	4.3	11.1	31.8	468.1	20.9	6.3	2.0	4.4	11.6	36.9	536.1	18.5	5.9	2.0	
8	4.4	12.3	36.3	370.4	30.8	9.3	2.8	4.4	12.3	37.1	409.6	31.2	9.3	2.8	4.4	12.4	38.3	454.3	31.2	9.3	2.8	4.4	12.9	42.5	556.3	30.4	9.1	2.8	
9	4.4	12.6	38.0	370.4	33.5	10.2	3.1	4.4	12.6	38.8	408.1	34.0	10.2	3.1	4.4	12.7	40.0	451.0	34.2	10.2	3.1	4.4	13.1	43.9	553.1	34.0	10.1	3.1	
10	4.0	11.1	32.9	370.4	29.7	9.4	3.1	4.0	11.1	33.6	411.3	30.1	9.4	3.1	4.0	11.2	34.5	458.7	30.4	9.4	3.1	4.0	11.6	37.7	575.0	30.6	9.4	3.1	
11	3.6	9.6	27.5	370.4	25.2	8.3	3.0	3.6	9.6	28.0	416.0	25.5	8.4	3.0	3.7	9.7	28.8	469.6	25.8	8.4	3.0	3.7	10.0	31.4	606.2	26.3	8.5	3.0	
12	3.4	8.5	23.5	370.4	21.7	7.5	2.9	3.4	8.5	23.9	420.7	22.0	7.5	2.9	3.4	8.6	24.5	480.9	22.3	7.6	2.9	3.4	8.8	26.7	639.4	22.9	7.7	2.9	
13	3.3	7.3	17.8	370.4	12.7	4.4	2.0	3.3	7.3	18.1	435.3	12.7	4.3	2.0	3.3	7.4	18.9	508.9	12.3	4.3	2.0	3.4	7.7	22.0	547.2	11.0	4.1	2.0	
14	3.4	7.9	20.0	370.4	15.0	5.1	2.0	3.5	7.9	20.4	429.5	14.9	5.0	2.0	3.5	8.0	21.2	498.0	14.7	5.0	2.0	3.5	8.3	24.4	584.1	13.4	4.8	2.0	
15	3.2	7.2	18.2	370.4	14.8	5.3	2.2	3.2	7.2	18.6	432.2	14.9	5.4	2.2	3.2	7.3	19.2	506.9	14.9	5.4	2.2	3.3	7.6	21.8	655.2	14.5	5.4	2.2	
16	3.0	6.4	15.7	370.4	13.3	5.1	2.3	3.0	6.4	15.9	438.6	13.4	5.1	2.3	3.0	6.5	16.4	523.5	13.5	5.2	2.3	3.0	6.8	18.5	720.9	13.6	5.3	2.3	
17	2.8	5.8	13.6	370.4	11.8	4.8	2.3	2.8	5.8	13.8	445.7	11.9	4.8	2.3	2.8	5.8	14.2	542.3	12.1	4.8	2.3	2.9	6.1	16.0	787.3	12.5	5.0	2.3	
		$(p_{+1}, \lambda, K) = (0.85, 0.72, 2.928)$																											
		$\kappa = 0$							$\kappa = 0.05$							$\kappa = 0.1$							$\kappa = 0.2$						
		$\delta$							$\delta$							$\delta$							$\delta$						
case		-0.5	-0.2	-0.1	0	0.1	0.2	0.5	-0.5	-0.2	-0.1	0	0.1	0.2	0.5	-0.5	-0.2	-0.1	0	0.1	0.2	0.5	-0.5	-0.2	-0.1	0	0.1	0.2	0.5
1	12.7	103.7	236.9	370.4	236.9	103.7	12.7	12.9	108.5	251.7	398.2	251.7	108.5	12.9	13.1	113.6	268.0	429.2	268.0	113.6	13.1	13.6	125.4	305.7	502.3	305.7	125.4	13.6	
2	7.3	68.2	192.9	370.4	192.7	68.1	7.3	7.4	71.5	207.1	406.0	206.9	71.4	7.4	7.5	75.3	223.3	446.8	223.0	75.2	7.5	7.7	84.5	262.1	547.4	261.8	84.4	7.7	
3	5.7	54.9	171.8	370.4	171.8	54.9	5.7	5.8	57.7	185.3	410.3	185.3	57.7	5.8	5.8	60.9	200.9	456.7	200.9	60.9	5.8	6.0	68.8	239.4	573.9	239.4	68.8	6.0	
4	4.6	44.7	152.8	370.4	152.8	44.7	4.6	4.7	47.0	165.6	414.7	165.6	47.0	4.7	4.7	49.7	180.6	466.9	180.6	49.7	4.7	4.9	56.5	218.3	602.1	218.3	56.5	4.9	
5	3.7	35.0	131.7	370.4	131.7	35.0	3.7	3.8	36.7	143.4	420.3	143.4	36.7	3.8	3.8	38.9	157.4	480.3	157.4	38.9	3.8	3.9	44.5	193.9	640.5	193.9	44.5	3.9	
6	3.2	28.0	114.3	370.4	114.3	28.0	3.2	3.2	29.4	125.0	425.7	125.0	29.4	3.2	3.2	31.2	138.1	493.6	138.1	31.2	3.2	3.3	35.9	173.0	680.1	173.0	35.9	3.3	
7	4.7	30.3	107.7	370.4	77.0	11.1	1.0	4.7	31.7	117.9	433.8	84.6	11.5	1.0	4.7	33.7	132.3	513.4	91.2	11.7	1.0	4.9	39.9	180.3	730.9	98.9	11.3	1.0	
8	4.8	36.6	128.1	370.4	111.1	23.2	1.8	4.8	38.4	139.6	423.8	121.5	24.3	1.8	4.9	40.8	154.5	488.9	132.6	25.5	1.8	5.0	47.5	198.3	664.5	156.0	27.9	1.8	
9	4.7	38.1	133.2	370.4	119.8	27.2	2.3	4.8	39.9	145.0	421.7	130.7	28.6	2.3	4.8	42.4	159.9	483.8	142.8	30.1	2.3	5.0	49.1	202.4	650.1	170.1	37.1	2.3	
10	3.9	31.3	117.9	370.4	107.3	23.4	2.2	3.9	32.8	128.8	426.2	117.5	24.6	2.3	4.0	34.8	142.8	494.8	129.2	25.9	2.3	4.1	40.5	183.1	683.4	156.9	29.2	2.3	
11	3.2	24.3	99.9	370.4	91.5	18.9	2.1	3.2	25.4	109.6	432.8	100.5	19.8	2.1	3.2	27.0	122.4	511.0	111.3	20.9	2.2	3.3	31.6	160.1	734.1	138.5	23.8	2.2	
12	2.7	19.3	85.0	370.4	78.2	15.4	2.0	2.7	20.2	93.7	439.4	86.2	16.1	2.0	2.8	21.5	105.2	527.9	96.1	17.0	2.0	2.8	25.3	140.5	789.4	122.5	19.6	2.1	
13	2.6	14.5	61.7	370.4	38.8	4.7	1.0	2.6	15.1	68.4	461.0	42.7	4.8	1.0	2.7	16.0	78.6	584.4	46.2	4.9	1.0	2.7	19.2	117.8	954.2	50.0	4.7	1.0	
14	2.8	16.9	71.1	370.4	49.0	6.6	1.0	2.8	17.6	78.6	452.5	54.1	6.8	1.0	2.9	18.7	89.7	561.9	59.1	6.9	1.0	2.9	22.3	129.6	889.0	66.7	7.0	1.0	
15	2.5	14.3	63.6	370.4	48.5	7.5	1.2	2.5	14.8	70.5	456.1	53.7	7.7	1.2	2.5	15.8	80.6	571.7	59.8	8.1	1.2	2.6	18.9	116.7	934.3	74.0	9.0	1.3	
16	2.1	11.1	52.2	370.4	41.5	6.8	1.3	2.1	11.5	58.0	465.2	46.1	7.0	1.3	2.1	12.2	66.7	596.7	52.0	7.3	1.3	2.2	14.7	98.8	1032.8	68.3	8.5	1.4	
17	1.9	8.8	42.7	370.4	34.7	5.9	1.3	1.9	9.1	47.5	475.6	38.6	6.0	1.3	1.9	9.7	55.1	626.0	44.0	6.4	1.3	2.0	11.6	83.9	1154.1	60.6	7.5	1.4	
		With the “flip a coin” strategy																											
		$(p_{+1}, \lambda, K) = (0.6, 0.12, 2.743)$																											
		$\kappa = 0$							$\kappa = 0.05$							$\kappa = 0.1$							$\kappa = 0.2$						
		$\delta$							$\delta$							$\delta$							$\delta$						
case		-0.5	-0.2	-0.1	0	0.1	0.2	0.5	-0.5	-0.2	-0.1	0	0.1	0.2	0.5	-0.5	-0.2	-0.1	0	0.1	0.2	0.5	-0.5	-0.2	-0.1	0	0.1	0.2	0.5
1	6.8	28.6	93.5	370.4	93.5	28.6	6.8	6.8	28.6	93.5	370.4	93.5	28.6	6.8	6.8	28.6	93.5	370.4	93.5	28.6	6.8	6.8	28.6	93.4	370.4	93.4	28.6	6.8	
2	5.3	19.3	64.3	370.4	64.2	19.3	5.3	5.3	19.3	64.3	370.4	64.2	19.3	5.3	5.3	19.3	64.3	370.4	64.2	19.3	5.3	5.3	19.4	64.6	370.4	64.5	19.4	5.3	
3	4.7	16.3	53.6	370.4	53.6	16.3	4.7	4.7	16.3	53.6	370.4	53.6	16.3	4.7	4.7	16.3	53.7	370.4	53.7	16.3	4.7	4.8	16.4	54.1	370.4	54.1	16.4	4.8	
4	4.3	14.0	45.4	370.4	45.4	14.0	4.3	4.3	14.0	45.4	370.4	45.4	14.0	4.3	4.3	14.0	45.5	370.4	45.5	14.0	4.3	4.4	14.2	46.0	370.4	46.0	14.2	4.4	
5	3.9	11.9	37.5	370.4	37.5	11.9	3.9	3.9	11.9	37.5	370.4	37.5	11.9	3.9	3.9	11.9	37.7	370.4	37.7	11.9	3.9	4.0	12.1	38.2	370.4	38.2	12.1	4.0	
6	3.6	10.4	31.8	370.4	31.8	10.4	3.6	3.6	10.4	31.8	370.4	31.8	10.4	3.6	3.6	10.5	32.0	370.4	32.0	10.5	3.6	3.7	10.6	32.6	370.4	32.6	10.6	3.7	
7	4.3	10.9	29.8	370.4	21.5	6.4	2.0	4.3	10.9	30.0	370.2	21.2	6.4	2.0	4.3	11.0	30.8	367.7	20.4	6.3	2.0	4.4	11.5	34.4	363.6	17.8	5.9	2.0	
8	4.4	12.3	36.3	370.4	30.8	9.3	2.8	4.4	12.3	36.5	3																		



**Table 6.** Vector of in-control probabilities  $(p'_{-1}, p'_0, p'_{+1})$  with the “flip a coin” strategy for the 17 distributions in Table 4.

case	$\kappa = 0$			$\kappa = 0.05$			$\kappa = 0.1$			$\kappa = 0.2$		
1	0.5000	0.0000	0.5000	0.5000	0.0000	0.5000	0.5000	0.0000	0.5000	0.5000	0.0000	0.5000
2	0.5000	0.0000	0.5000	0.5000	0.0000	0.5000	0.5000	0.0000	0.5000	0.5000	0.0000	0.5000
3	0.5000	0.0000	0.5000	0.5000	0.0000	0.5000	0.5000	0.0000	0.5000	0.5000	0.0000	0.5000
4	0.5000	0.0000	0.5000	0.5000	0.0000	0.5000	0.5000	0.0000	0.5000	0.5000	0.0000	0.5000
5	0.5000	0.0000	0.5000	0.5000	0.0000	0.5000	0.5000	0.0000	0.5000	0.5000	0.0000	0.5000
6	0.5000	0.0000	0.5000	0.5000	0.0000	0.5000	0.5000	0.0000	0.5000	0.5000	0.0000	0.5000
7	0.5000	0.0000	0.5000	0.4996	0.0000	0.5004	0.4986	0.0000	0.5014	0.4942	0.0000	0.5058
8	0.5000	0.0000	0.5000	0.4999	0.0000	0.5001	0.4994	0.0000	0.5006	0.4976	0.0000	0.5024
9	0.4999	0.0000	0.5001	0.4998	0.0000	0.5002	0.4995	0.0000	0.5005	0.4982	0.0000	0.5018
10	0.5000	0.0000	0.5000	0.4999	0.0000	0.5001	0.4996	0.0000	0.5004	0.4984	0.0000	0.5016
11	0.5000	0.0000	0.5000	0.4999	0.0000	0.5001	0.4996	0.0000	0.5004	0.4985	0.0000	0.5015
12	0.5000	0.0000	0.5000	0.4999	0.0000	0.5001	0.4996	0.0000	0.5004	0.4985	0.0000	0.5015
13	0.5000	0.0000	0.5000	0.4994	0.0000	0.5006	0.4978	0.0000	0.5022	0.4912	0.0000	0.5088
14	0.4999	0.0000	0.5001	0.4995	0.0000	0.5005	0.4983	0.0000	0.5017	0.4932	0.0000	0.5068
15	0.5000	0.0000	0.5000	0.4997	0.0000	0.5003	0.4987	0.0000	0.5013	0.4950	0.0000	0.5050
16	0.5000	0.0000	0.5000	0.4997	0.0000	0.5003	0.4989	0.0000	0.5011	0.4957	0.0000	0.5043
17	0.5000	0.0000	0.5000	0.4997	0.0000	0.5003	0.4989	0.0000	0.5011	0.4959	0.0000	0.5041

in Table 5(bottom) we can conclude that:

- For symmetric distributions, no matter the value of  $\kappa$  and the pair of  $(\lambda, K)$ , the “the flip a coin” strategy guarantees that our proposed nonparametric control chart almost maintains its distribution-free property. On the other hand, if we do not use the “the flip a coin” strategy we proved that the chart is no longer distribution-free.
- Regarding the choice of the pair  $(\lambda, K)$  it seems that using larger values of  $\lambda$ , except from cases 14 and 15 improves significantly the distribution-free property of our chart for heavy-tailed distributions (cases 13 – 17) and large values of  $\kappa$ . For example for  $\kappa = 0.2$  using  $(\lambda, K) = (0.12, 2.743)$  the in-control ARL value for case 16 is  $ARL = 347.5$  and for case 17 is  $ARL = 350$ . On the other hand, using the pair  $(\lambda, K) = (0.72, 2.928)$ , the in-control ARL value for case 16 is  $ARL = 365.8$  and for case 17 is  $ARL = 366.3$ .
- Similarly, for the out-of-control cases, we can conclude that no matter the value of  $\kappa$  the  $ARL_1$  values are almost the same. For example, when  $\delta = 0.1$  using  $(\lambda, K) = (0.72, 2.928)$  for  $\kappa = \{0, 0.05, 0.1, 0.2\}$  the corresponding  $ARL_1 = \{78.2, 78.2, 78.2, 78.5\}$ .

#### 4.3. Performance evaluations

The performance of the C-SN EWMA chart under the “flip a coin strategy” will be compared with the Shewhart Sign chart presented in [4] under the Benchmark of the distributions listed in Table 4. As far as we are concerned, these are the only two existing schemes dealing with rounding-off errors. In Table 7 the corresponding  $ARL_1$  values are presented for  $n = 20$  for both charts. In order to perform fair comparisons since for the Shewhart chart the closest  $ARL_0$  value to 370.4 is  $ARL_0 \approx 388.1$  when the control limit equals  $C = 14$ , our chart will be optimized in order to also verify  $ARL_0 = 388.1$ . More specifically, for a fixed value of  $\lambda$  the corresponding value of  $K$  will be computed such that it gives  $ARL_0 = 388.1$  when  $\kappa = 0$ . Finally the same optimal pair of  $(\lambda, K)$  will be used in order to compute the chart’s performance for  $\kappa = \{0.05, 0.1, 0.2\}$ . Note that, as presented above, setting  $\lambda > 0.7$  guarantees an approximately distribution-free behaviour for the C-SN EWMA chart. So it would be logical to optimize  $\lambda$  also. Nevertheless, it is not necessary to do this since, even by setting  $\lambda = 0.7$ , our chart outperforms the Shewhart chart. In particular, from Table

7 we may conclude that our chart performs better for any shift magnitude regardless the underlying distribution or the value of  $\kappa$ . For instance, for cases #6,#7,#8, when the shift magnitude is  $\delta = 0.2$  and  $\kappa = 0.2$  the corresponding ARL<sub>1</sub> values of the Sign Shewhart chart are 56.9, 18.4, 44, 4 respectively. On the other hand, for the same cases, the corresponding ARL<sub>1</sub> values of the C-SN EWMA chart are 28.4, 8.9, 21.6.

**Table 7.** Performance comparisons between the C-SN EWMA and the Shewhart Sign charts under the “flip a coin” strategy for  $n = 20$

		C-SN EWMA chart																							
		$\kappa = 0$						$\kappa = 0.05$						$\kappa = 0.1$						$\kappa = 0.2$					
		$\delta$						$\delta$						$\delta$						$\delta$					
		-0.5	-0.2	-0.1	0.1	0.2	0.5	-0.5	-0.2	-0.1	0.1	0.2	0.5	-0.5	-0.2	-0.1	0.1	0.2	0.5	-0.5	-0.2	-0.1	0.1	0.2	0.5
1	12.40	103.90	243.20	243.20	103.90	12.40	12.40	103.90	243.20	243.20	103.90	12.40	12.40	103.80	243.20	243.20	103.80	12.40	12.40	103.80	243.10	243.10	103.80	12.40	
2	7.10	67.60	196.60	196.40	67.60	7.10	7.10	67.70	196.60	196.40	67.60	7.10	7.10	67.70	196.70	196.50	67.70	7.10	7.20	68.10	197.20	197.00	68.00	7.20	
3	5.60	54.30	174.40	174.40	54.30	5.60	5.60	54.40	174.40	174.40	54.40	5.60	5.60	54.50	174.60	174.60	54.50	5.60	5.70	54.90	175.40	175.40	54.90	5.70	
4	4.60	44.10	154.60	154.60	44.10	4.60	4.60	44.10	154.70	154.70	44.10	4.60	4.60	44.30	154.90	154.90	44.30	4.60	4.60	44.80	156.00	156.00	44.80	4.60	
5	3.70	34.30	132.60	132.60	34.30	3.70	3.70	34.40	132.80	132.80	34.40	3.70	3.70	34.60	133.20	133.20	34.60	3.70	3.80	35.20	134.70	134.70	35.20	3.80	
6	3.10	27.50	114.70	114.70	27.50	3.10	3.10	27.50	114.90	114.90	27.50	3.10	3.20	27.70	115.40	115.40	27.70	3.20	3.20	28.40	117.30	117.30	28.40	3.20	
7	4.60	29.70	107.90	76.60	10.80	1.00	4.60	29.90	108.80	75.50	10.70	1.00	4.60	30.40	111.60	72.40	10.30	1.00	4.70	32.30	123.30	61.20	8.90	1.00	
8	4.70	36.00	129.00	111.40	22.70	1.80	4.70	36.10	129.60	110.90	22.60	1.80	4.70	36.50	131.30	109.40	22.40	1.80	4.80	38.10	138.50	103.70	21.60	1.80	
9	4.70	37.40	134.20	120.30	26.70	2.30	4.70	37.50	134.70	120.00	26.60	2.30	4.70	37.90	136.10	119.00	26.50	2.30	4.80	39.30	142.00	115.00	26.00	2.30	
10	3.90	30.60	118.40	107.60	22.90	2.30	3.90	30.70	118.80	107.40	22.90	2.30	3.90	31.00	120.20	106.70	22.90	2.30	4.00	32.30	125.60	104.30	22.80	2.30	
11	3.20	23.80	99.90	91.30	18.40	2.10	3.20	23.80	100.40	91.20	18.40	2.10	3.20	24.10	101.60	91.00	18.50	2.10	3.20	25.20	106.90	90.10	18.80	2.10	
12	2.70	18.90	84.80	77.80	15.00	2.00	2.70	18.90	85.20	77.80	15.00	2.00	2.70	19.20	86.40	77.80	15.20	2.00	2.80	20.20	91.60	78.10	15.60	2.00	
13	2.60	14.10	61.20	38.10	4.70	1.00	2.60	14.20	61.90	37.50	4.60	1.00	2.60	14.50	64.20	35.60	4.50	1.00	2.70	15.80	74.70	29.40	4.10	1.00	
14	2.80	16.40	70.60	48.40	6.40	1.00	2.80	16.50	71.30	47.80	6.40	1.00	2.80	16.90	73.60	46.00	6.30	1.00	2.90	18.20	83.40	39.80	5.90	1.00	
15	2.50	13.90	63.10	47.80	7.30	1.20	2.50	14.00	63.70	47.60	7.30	1.20	2.50	14.30	65.60	46.90	7.40	1.20	2.50	15.40	73.90	44.50	7.50	1.30	
16	2.10	10.80	51.60	40.90	6.60	1.30	2.10	10.90	52.10	40.90	6.70	1.30	2.10	11.10	53.80	40.80	6.70	1.30	2.20	12.10	61.20	40.80	7.10	1.40	
17	1.90	8.60	42.10	34.10	5.70	1.30	1.90	8.70	42.60	34.20	5.80	1.30	1.90	8.90	44.20	34.50	5.90	1.30	1.90	9.80	51.00	35.90	6.40	1.40	

		Shewhart Sign chart																							
		$\kappa = 0$						$\kappa = 0.05$						$\kappa = 0.1$						$\kappa = 0.2$					
		$\delta$						$\delta$						$\delta$						$\delta$					
		-0.5	-0.2	-0.1	0.1	0.2	0.5	-0.5	-0.2	-0.1	0.1	0.2	0.5	-0.5	-0.2	-0.1	0.1	0.2	0.5	-0.5	-0.2	-0.1	0.1	0.2	0.5
1	25.90	164.70	296.10	296.10	164.70	25.90	25.90	164.70	296.10	296.10	164.70	25.90	25.90	164.60	296.10	296.10	164.60	25.90	25.90	164.60	296.10	296.10	164.60	25.90	
2	14.30	118.20	258.40	258.20	118.10	14.30	14.30	118.30	258.40	258.20	118.20	14.30	14.30	118.40	258.50	258.30	118.30	14.30	14.40	118.80	259.00	258.70	118.70	14.40	
3	10.70	99.00	238.40	238.40	99.00	10.70	10.80	99.10	238.50	238.50	99.10	10.80	10.80	99.20	238.70	238.70	99.20	10.80	10.90	99.90	239.40	239.40	99.90	10.90	
4	8.30	83.30	219.50	219.50	83.30	8.30	8.30	83.30	219.60	219.60	83.30	8.30	8.40	83.50	219.90	219.90	83.50	8.40	8.50	84.40	221.00	221.00	84.40	8.50	
5	6.30	67.30	197.00	197.00	67.30	6.30	6.30	67.40	197.20	197.20	67.40	6.30	6.30	67.60	197.60	197.60	67.60	6.30	6.40	68.70	199.20	199.20	68.70	6.40	
6	5.00	55.20	177.30	177.30	55.20	5.00	5.00	55.40	177.50	177.50	55.40	5.00	5.00	55.70	178.00	178.00	55.70	5.00	5.10	56.90	180.20	180.20	56.90	5.10	
7	8.30	59.30	169.50	130.40	22.60	1.00	8.30	59.60	170.50	129.00	22.30	1.00	8.40	60.40	173.70	124.80	21.40	1.00	8.60	63.80	186.90	109.10	18.40	1.00	
8	8.60	70.10	193.10	173.50	46.40	2.10	8.70	70.30	193.70	172.90	46.30	2.10	8.70	70.90	195.60	171.20	45.90	2.10	8.80	73.50	203.20	164.40	44.40	2.20	
9	8.50	72.50	198.70	183.60	53.80	3.00	8.50	72.60	199.20	183.20	53.70	3.00	8.60	73.20	200.70	182.10	53.50	3.00	8.80	75.50	206.80	177.60	52.50	3.10	
10	6.70	60.90	181.40	169.00	46.90	3.00	6.70	61.10	181.90	168.80	46.90	3.00	6.70	61.60	183.40	168.10	46.80	3.00	6.90	63.80	189.40	165.20	46.70	3.10	
11	5.00	48.50	160.00	149.40	38.20	2.70	5.00	48.60	160.50	149.30	38.30	2.70	5.10	49.10	162.00	149.00	38.40	2.70	5.20	51.20	168.20	147.90	38.90	2.80	
12	4.00	39.10	141.10	132.00	31.40	2.40	4.00	39.30	141.60	132.00	31.50	2.40	4.00	39.80	143.30	132.10	31.70	2.50	4.10	41.80	149.80	132.40	32.60	2.60	
13	2.80	18.00	71.60	29.80	1.60	1.00	2.80	18.10	72.80	28.60	1.60	1.00	2.80	18.60	76.70	25.10	1.50	1.00	2.90	20.90	95.00	15.20	2.00	1.00	
14	3.80	29.50	109.00	73.60	8.50	1.00	3.80	29.70	110.10	72.50	8.40	1.00	3.80	30.30	113.40	69.50	8.20	1.00	3.90	32.90	127.80	58.60	7.30	1.00	
15	4.20	34.30	122.30	90.00	12.70	1.00	4.20	34.50	123.30	89.10	12.60	1.00	4.30	35.10	126.30	86.30	12.30	1.00	4.40	37.80	139.30	76.40	11.30	1.00	
16	3.40	29.10	111.80	89.20	14.70	1.20	3.50	29.30	112.70	88.80	14.70	1.20	3.50	29.90	115.40	87.70	14.80	1.20	3.60	32.20	126.70	83.90	15.10	1.30	
17	2.70	22.50	94.90	78.10	13.10	1.40	2.70	22.70	95.70	78.10	13.20	1.40	2.70	23.20	98.30	78.00	13.40	1.40	2.80	25.30	109.10	78.00	14.30	1.40	
18	2.30	17.60	80.00	66.80	11.10	1.40	2.30	17.80	80.80	67.00	11.20	1.40	2.30	18.30	83.40	67.60	11.40	1.40	2.30	20.20	94.00	69.90	12.60	1.40	

**5. An illustrative example**

In this Section a modified version of the example originally discussed by Celano et al. in [6] is provided, to show a practical Phase II implementation of the design and operation of our proposed chart under the case of measurement error. In this example, the quality characteristic to be monitored is the radial error, defined as “a quality characteristic frequently monitored in hole drilling processes of mechanical parts and assembly processes of printed circuit boards”. At each sampling point  $t$ , a subgroup of size  $n = 20$  is collected in order to detect a shift in the median of the quality characteristic of interest such that  $p_0 = 0.5$  shifts to  $p_1 = 0.7$ . Additionally, as shown in [6] the in-control value of the median for the radial error is  $\theta_0 = 0.338$ . The original dataset is presented in Table 8 (top). For illustration purposes let us assume that the practitioner does not have at his disposal the true values due to a rounding-off error in the measurement system (the resolution value is  $\rho = 0.05$ ), and through the model presented in equation (10), obtains the values presented in Table 8 (bottom). Similarly the observed value of the median will be  $\theta'_0 = 0.3$  instead of the true one  $\theta_0 = 0.338$ .

Moreover, in Table 8 (top) the corresponding values of  $S_{t,j} = \text{sign}(X'_{t,j} - \theta'_0)$  are presented. In can be clearly seen that due to the rounding-off error in the measurement system many ties occur (zero values for  $S_{t,j}$ ). In order to overcome

this problem we will use the “flip a coin” method presented in Section 4.2. More specifically, each  $S_{t,j} = 0$  will be substituted by  $S'_{t,j} = 2\Delta_{t,j} - 1$  where  $\Delta_{t,j}$  will be a random number generated from  $\text{Ber}(0.5)$ . These values are presented in Table 8 (bottom) along with the corresponding values of  $\text{SN}_t, \text{SN}_t^*$  and  $Z_t^*$ . Additionally, for the design of the chart’s parameters we used  $\lambda^* = 0.305, K^* = 2.903$  (as the optimal pair for detecting a shift  $p_{+1} = 0.7$  when  $n = 20$ ),  $\sigma = 0.2$  (“continuousify” parameter) and  $Z_0^* = 0$  (no head-start feature). Then, by substituting these values in equations (8) and (9), we obtain the values of the control limits for the two-sided C-SN EWMA chart as  $\text{LCL}^* = -5.5127, \text{UCL}^* = 5.5127$ .

It should be pointed out that even though the operation of this chart requires random numbers to be generated, its Run Length properties (such as ARL, SDRL), are obtained directly through the distribution of the  $\text{SN}_t^*$  with the exact Markov chain method shown in Section 2.1 without the need of performing any simulations. This fact has been also mentioned in [28]. Finally, the values of the charting statistic  $Z_t^*$  are plotted in Figure 1. It can be seen that at the 4<sup>th</sup> sampling point ( $t = 4$ ) an out-of-control signal is given stating that the process median has changed.

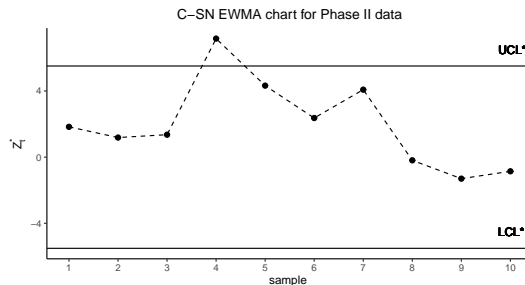


**Figure 1.** Radial error example: the C-SN EWMA chart for the Phase II data presented in Table 8 (bottom)

## 6. Conclusions

In this paper we proposed a modified distribution-free EWMA control chart based on the Sign statistic called as the C-SN EWMA chart. Using the “continuousify” method originally introduced in [28] we determined its RL properties showing that the results are not affected by the number of subintervals. It is worth stretching that, its in- and out-of-control performances were computed regardless of the process underlying distribution. Additionally, we examined how seriously the rounding-off error affects the distribution-free properties of the EWMA Sign control chart. Under a benchmark of 17 Johnson’s type distributions we proved that, when ties occur, a conventional nonparametric EWMA chart based on the Sign statistic is no longer distribution-free. The solution we opted was based on a Bernoulli trial approach, originally introduced in [4], which turns out to be a very efficient method to maintain the distribution-free property for our proposed C-SN EWMA control chart and it is applicable to any situation. Finally, the performance of our proposed chart was examined by comparing it with the Shewhart Sign chart introduced in [4] and the superiority of our scheme was proven for any shift magnitude.

**Table 8.** Radial error example: Phase II sample of  $t = 1, \dots, 10$  subgroups of size  $n = 20$  for the true values (top) and the observed values (bottom) along with the  $S_{t,j}$  values with and without the "flip a coin strategy" when  $\rho = 0.05$

Without the "flip a coin" strategy																				
t	$X_{t,j}$ true values																			
	1	2	3	4	5	6	7	8	9	10	11	12	13	14	15	16	17	18	19	20
1	0.289	0.380	0.483	0.288	0.544	0.390	0.567	0.512	0.433	0.168	0.128	0.428	0.081	0.575	0.396	0.574	0.730	0.407	0.367	0.452
2	0.447	0.599	0.207	0.317	0.256	0.433	0.218	0.329	0.432	0.674	0.233	0.570	0.748	0.364	0.372	0.798	0.218	0.405	0.060	0.632
3	0.081	0.368	0.435	0.216	0.246	0.229	0.623	0.455	0.394	0.616	0.116	0.611	0.666	0.262	0.410	0.234	0.692	0.719	1.033	0.376
4	0.954	0.537	0.621	0.513	1.540	0.609	0.801	1.080	1.069	0.954	0.852	0.425	1.389	0.794	1.081	0.900	0.521	0.576	0.761	0.535
5	0.316	0.237	0.286	0.879	0.190	0.104	0.570	0.448	0.269	0.746	0.344	0.191	0.366	0.315	0.408	0.522	0.598	0.232	0.671	0.448
6	0.342	0.378	0.287	0.328	0.589	0.233	0.255	0.119	0.284	0.499	0.410	0.668	0.385	0.594	0.390	0.265	0.409	0.434	0.628	0.316
7	0.370	0.391	0.525	0.459	1.280	0.470	0.482	0.032	0.525	0.628	0.686	0.584	0.300	0.245	0.555	0.113	0.194	0.932	0.597	0.523
8	0.352	0.264	0.759	0.154	0.256	0.426	0.363	0.310	0.303	0.316	0.807	0.235	0.173	0.183	1.105	0.068	0.368	0.736	0.097	0.060
9	0.305	0.352	0.468	0.224	0.739	0.234	0.171	0.250	0.308	0.431	0.092	0.326	0.455	0.569	0.354	0.475	0.530	0.312	0.102	0.651
10	0.603	0.363	0.628	0.314	0.029	0.436	0.207	0.553	0.645	0.122	0.759	0.296	0.691	0.425	0.441	0.323	0.287	0.310	0.194	0.582
With the "flip a coin" strategy																				
t	$X'_{t,j}$ observed values when $\rho = 0.05$																			
	1	2	3	4	5	6	7	8	9	10	11	12	13	14	15	16	17	18	19	20
1	0.30	0.40	0.50	0.30	0.55	0.40	0.55	0.50	0.45	0.15	0.15	0.45	0.10	0.55	0.40	0.55	0.75	0.40	0.35	0.45
2	0.45	0.60	0.20	0.30	0.25	0.45	0.20	0.35	0.45	0.65	0.25	0.55	0.75	0.35	0.35	0.80	0.20	0.40	0.05	0.65
3	0.10	0.35	0.45	0.20	0.25	0.25	0.60	0.45	0.40	0.60	0.10	0.60	0.65	0.25	0.40	0.25	0.70	0.70	1.05	0.40
4	0.95	0.55	0.60	0.50	1.55	0.60	0.80	1.10	1.05	0.95	0.85	0.45	1.40	0.80	1.10	0.90	0.50	0.60	0.75	0.55
5	0.30	0.25	0.30	0.90	0.20	0.10	0.55	0.45	0.25	0.75	0.35	0.20	0.35	0.30	0.40	0.50	0.60	0.25	0.65	0.45
6	0.35	0.40	0.30	0.35	0.60	0.25	0.25	0.10	0.30	0.50	0.40	0.65	0.40	0.60	0.40	0.25	0.40	0.45	0.65	0.30
7	0.35	0.40	0.55	0.45	1.30	0.45	0.50	0.05	0.55	0.65	0.70	0.60	0.30	0.25	0.55	0.10	0.20	0.95	0.60	0.50
8	0.35	0.25	0.75	0.15	0.25	0.45	0.35	0.30	0.30	0.30	0.80	0.25	0.15	0.20	1.10	0.05	0.35	0.75	0.10	0.05
9	0.30	0.35	0.45	0.20	0.75	0.25	0.15	0.25	0.30	0.45	0.10	0.35	0.45	0.55	0.35	0.45	0.55	0.30	0.10	0.65
10	0.60	0.35	0.65	0.30	0.05	0.45	0.20	0.55	0.65	0.10	0.75	0.30	0.70	0.45	0.45	0.30	0.30	0.30	0.20	0.60
t	$S'_{t,j}$ values using the "flip a coin strategy" along with the corresponding $SN_t, SN'_t, Z'_t$ values																			
	$S'_{t,j} = \text{sign}(X'_{t,j} - \theta'_0)$																			
1	-1	1	1	-1	1	1	1	1	1	1	-1	-1	1	-1	1	1	1	1	-1	1
2	1	1	-1	-1	-1	1	-1	-1	-1	1	1	-1	1	1	-1	1	1	-1	1	-1
3	-1	1	1	-1	-1	-1	-1	1	1	1	1	-1	1	1	-1	1	-1	1	1	1
4	1	1	1	1	1	1	1	1	1	1	1	1	1	1	1	1	1	1	1	1
5	-1	-1	-1	1	-1	-1	-1	1	-1	1	-1	-1	-1	-1	1	1	1	-1	1	1
6	1	1	-1	1	1	-1	-1	-1	-1	1	1	1	1	1	1	-1	1	1	1	-1
7	-1	1	1	1	1	1	1	-1	1	1	1	1	-1	-1	1	-1	-1	1	1	1
8	-1	-1	1	-1	-1	1	1	1	-1	-1	-1	1	-1	-1	1	-1	-1	-1	1	-1
9	-1	1	1	-1	1	-1	-1	-1	-1	-1	1	-1	-1	1	1	-1	1	1	-1	1
10	1	1	1	-1	-1	1	-1	1	1	1	-1	1	-1	1	1	1	-1	-1	-1	1
	$SN_t$	$SN'_t$	$Z'_t$																	
1	8	7.8729	2.4012																	
2	2	1.6446	2.1705																	
3	6	6.1533	3.3853																	
4	20	20.0549	8.4695																	
5	-2	-2.0159	5.2715																	
6	6	6.0806	5.5183																	
7	8	7.9114	6.2482																	
8	-8	-7.7615	1.9752																	
9	-2	-2.2089	0.6991																	
10	2	1.8322	1.0447																	

As a future work many things can be pursued. For instance, the “continuousify” method could be applied in EWMA-type schemes where other nonparametric statistics are considered such as the Mann-Whitney, and the Ansari-Bradley statistics with and without ties. Additionally, it would be interesting to examine the performance of an EWMA chart based on the Wilcoxon Signed Rank statistic in the presence of ties in the population. Finally, a challenging problem would be to investigate the use of kernel-based techniques in distribution-free EWMA schemes designed for monitoring bivariate processes.

## Acknowledgments

The authors would like to express their gratitude to the Editor and the two anonymous reviewers for their constructive comments which improved the content and the presentation of this paper.

## References

- [1] V. Alevizakos, C. Koukouvinos, and K. Chatterjee, *A Nonparametric Double Generally Weighted Moving Average Signed-Rank Control Chart for Monitoring Process Location*, Quality and Reliability Engineering International 7 (2020), pp. 2441–2458.
- [2] R. Amin and A. Searcy, *A Nonparametric Exponentially Weighted Moving Average Control Scheme*, Communications in Statistics-Simulation and Computation 20 (1991), pp. 1049–1072.
- [3] D. Brook and D. Evans, *An Approach to the Probability Distribution of CUSUM Run Length*, Biometrika 59 (1972), pp. 539–549.
- [4] P. Castagliola, K. Tran, G. Celano, and P. Maravelakis, *The Shewhart Sign Chart with Ties: Performance and Alternatives*, in *Distribution-Free Methods for Statistical Process Monitoring and Control*, Springer, 2020, pp. 107–136.
- [5] P. Castagliola, K. Tran, G. Celano, A. Rakitzis, and P. Maravelakis, *An EWMA-Type Sign Chart With Exact Run Length Properties*, Journal of Quality Technology 51 (2019), pp. 51–63.
- [6] G. Celano, P. Castagliola, S. Chakraborti, and G. Nenes, *On the Implementation of the Shewhart Sign Control Chart for Low-volume Production*, International Journal of Production Research 54 (2016), pp. 5886–5900.
- [7] S. Chakraborti and M. Graham, *Nonparametric (Distribution-Free) Control Charts: An Updated Overview and Some Results*, Quality Engineering 31 (2019), pp. 523–544.
- [8] N. Chakraborty, S. Chakraborti, S. Human, and N. Balakrishnan, *A Generally Weighted Moving Average Signed-Sank Control Chart*, Quality and Reliability Engineering International 32 (2016), pp. 2835–2845.
- [9] C.W. Champ and S.E. Rigdon, *A a comparison of the markov chain and the integral equation approaches for evaluating the run length distribution of quality control charts*, Communications in Statistics-Simulation and Computation 20 (1991), pp. 191–204.
- [10] S.v. Crowder, *A simple method for studying run-length distributions of exponentially weighted moving average charts*, Technometrics 29 (1987), pp. 401–407.
- [11] D.Y. Fong, C. Kwan, K. Lam, and K.S.L. Lam, *Use of the Sign Test for the Median in the Presence of Ties*, The American Statistician 57 (2003), pp. 237–240.
- [12] J. Gibson and J. Melsa, *Introduction to Nonparametric Detection with Applications*, Academic press, 1976.
- [13] M. Graham, S. Chakraborti, and S. Human, *A Nonparametric EWMA Sign Chart for Location Based on Individual Measurements*, Quality Engineering 23 (2011), pp. 227–241.

- [14] M. Graham, S. Chakraborti, and S. Human, *A Nonparametric Exponentially Weighted Moving Average Signed-Rank Chart for Monitoring Location*, Computational Statistics & Data Analysis 55 (2011), pp. 2490–2503.
- [15] A. Haq, *A New Nonparametric Synthetic EWMA Control Chart for Monitoring Process Mean*, Communications in Statistics-Simulation and Computation 48 (2019), pp. 1665–1676.
- [16] G. Latouche and V. Ramaswami, *Introduction to Matrix Analytic Methods in Stochastic Modeling*, ASA-SIAM, Philadelphia, 1999.
- [17] K. Linna and W. Woodall, *Effect of Measurement Error on Shewhart Control Charts*, Journal of Quality technology 33 (2001), pp. 213–222.
- [18] M. Maleki, A. Amiri, and P. Castagliola, *Measurement Errors in Statistical Process Monitoring: A Literature Review*, Computers & Industrial Engineering 103 (2017), pp. 316–329.
- [19] D. Montgomery, *Introduction to Statistical Quality Control*, John Wiley & Sons, 2020.
- [20] M. Neuts, *Matrix-Geometric Solutions in Stochastic Models: An Algorithmic Approach*, Dover Publications Inc, New York, 1981.
- [21] M. Nojavan, M. Alishahi, M. Rezaee, and M.A. Rahae, *The Effect of Measurement Error on the Performance of Mann-Whitney and Signed-Rank Nonparametric Control Charts*, Quality and Reliability Engineering International (2021).
- [22] E. Page, *Continuous Inspection Schemes*, Biometrika 41 (1954), pp. 100–115.
- [23] T. Perdakis, S. Psarakis, P. Castagliola, and P. Maravelakis, *An EWMA Signed Ranks Control Chart with Reliable Run Length Performances*, Quality and Reliability Engineering International 37 (2021), pp. 1266–1284.
- [24] J. Putter, *The Treatment of Ties in Some Nonparametric Tests*, The Annals of Mathematical Statistics 26 (1955), pp. 368–386.
- [25] M. Riaz, *A Sensitive Non-Parametric EWMA Control Chart*, Journal of the Chinese Institute of Engineers 38 (2015), pp. 208–219.
- [26] S. Roberts, *Control Chart Tests Based on Geometric Moving Averages*, Technometrics 1 (1959), pp. 239–250.
- [27] W. Shewhart, *Quality Control Charts*, The Bell System Technical Journal 5 (1926), pp. 593–603.
- [28] S. Wu, P. Castagliola, and G. Celano, *A Distribution-free EWMA Control Chart for Monitoring Time-Between-Events-and-Amplitude Data*, Journal of Applied Statistics 3 (2020), pp. 434–454.
- [29] S.F. Yang, J.S. Lin, and S. Cheng, *A New Nonparametric EWMA Sign Control Chart*, Expert Systems with Applications 38 (2011), pp. 6239–6243.